Evaluating robustness of harvest control rules to climate-driven variability in Pacific sardine recruitment

Robert P. Wildermuth [a,b], Desiree Tommasi [a,b], Peter Kuriyama [b], James Smith[a,b], and Isaac Kaplan [c]

[a]University of California, Santa Cruz, Institute of Marine Sciences' Fisheries Collaborative Program, 1156 High Street, Santa Cruz, CA 95064, USA; [b]Fisheries Resources Division, Southwest Fisheries Science Center, National Marine Fisheries Service, National Oceanic and Atmospheric Administration, 8901 La Jolla Shores Drive, La Jolla, CA 92037, USA; [c]Conservation Biology Division, Northwest Fisheries Science Center, National Marine Fisheries Service, National Oceanic and Atmospheric Administration, 2725 Montlake Boulevard, East Seattle, WA 98112, USA

Corresponding author: **Robert P. Wildermuth** (email: Robert.Wildermuth@noaa.gov)

Abstract

Climate-driven changes in ocean temperatures, currents, or plankton dynamics may disrupt pelagic forage fish recruitment. Being responsive to such impacts enables fisheries management to ensure continued sustainable harvest of forage species. We conducted a management strategy evaluation to assess the robustness of current and alternative Pacific sardine harvest control rules under a variety of recruitment scenarios representing potential projections of future climate conditions in the California Current. The current environmentally informed control rule modifies the harvest rate for the northern sardine subpopulation based on average sea surface temperatures measured during California Cooperative Oceanic Fisheries Investigations field cruises. This rule prioritizes catch at intermediate biomass levels but may increase variability in catch and closure frequency compared to alternative control rules, especially if recruitment is unrelated to ocean temperatures. Fishing at maximum sustainable yield and using dynamically estimated reference points reduced the frequency of biomass falling below 150 000 mt by up to 17%, while using survey index-based biomass estimates resulted in a 14% higher risk of delayed fishery closure during stock declines than when using assessment-based estimates.

Key words: management strategy evaluation, fisheries management, *Sardinops sagax*, performance evaluation

Introduction

Small pelagic forage fishes provide the fundamental ecosystem services of linking primary production to larger, commercially desirable predator species and delivering essential nutrients to predators and fisheries markets alike (Pikitch et al. 2012, 2014). In 2020, forage finfishes directly supported a 10.1 billion USD industry for global markets (FAO 2022), and analyses by Pikitch et al. (2014) suggest these fish provide supporting services as forage to harvested predator species worth twice that value (roughly an additional 20.3 billion USD globally). Further, this global market value is an underestimate as it does not account for support services as bait for wild capture fisheries, recreational and subsistence catch of forage fishes, nor as prey for protected species like marine mammals and seabirds (Pikitch et al. 2014, see also Konar et al. 2019). Because of their importance for supporting higher trophic level species and their respective population recoveries, many proposals to conserve forage stocks have been presented, though predator reliance on harvested forage fishes may not necessitate full moratoria on these fisheries (Cury et al. 2011; Kaplan et al. 2013; Koehn et al. 2017, 2021; Free et al. 2021).

Forage fish likely have complex and dynamic biological properties that complicate observation and assessment of stocks. A primary characteristic of forage species is large and rapid population fluctuations in the absence of commercial exploitation (Baumgartner et al. 1992; Schwartzlose et al. 1999; McClatchie et al. 2017; Salvatteci et al. 2018). These boom–bust cycles can span multiple years and orders of magnitude in terms of biomass (Chavez et al. 2003). Although collapses can be exacerbated by fishing mortality, relatively short lifespans and high reproductive output means that recruitment success or failure drives these boom–bust dynamics for most forage fish populations (Essington et al. 2015; Szuwalski and Hilborn 2015; Checkley et al. 2017). Though the exact drivers of recruitment in marine fishes continue to be debated (Zwolinski and Demer 2014, 2019), ecological theory, modeling, and observations suggest that this recruitment variability is ultimately due to environmental factors (Hjort 1914; Houde 1987; Cowan and Shaw 2002; Brosset et al. 2020).

Despite their importance in the ecosystem, forage fish life history characteristics make it a challenge to observe and assess their population dynamics. Due to the migratory and aggregation behavior of forage fishes, surveys must be

extensive (e.g., Hewitt 1988) or make assumptions about availability of fish to these surveys to estimate distribution and density of stocks (Pitcher 1995; Zwolinski et al. 2011). In the highly dynamic and productive systems in which these fishes are found, many environmental factors influence their distribution, growth, and survival (Jacobson and Mac-Call 1995; Fiechter et al. 2015; Checkley et al. 2017), as well as their detection by surveys (Zwolinski et al. 2011). While many environmental influences on forage fish productivity have been proposed (e.g., Rykaczewski and Checkley 2008; Zwolinski and Demer 2014), few have been operationalized in formal fisheries management frameworks. This in no small part is due to the crucial requirement of an accurate and predictable environmental index on which to base predictions about future stock dynamics (Basson 1999). However, advances in climate modeling have improved our ability to project regional conditions at ecologically significant scales. These advances, combined with modern computing capacity, lay a path for long-term evaluations of forage fish stock dynamics in response to fisheries management decisions and climate change.

Faced with this variability, the short life-cycle of forage fish stocks, and their importance for human use and to marine predators, fisheries managers rely on frequent pre-season surveys (e.g., de Moor 2018) and (or) short-term projections of forage fish biomass from modern stock assessment models (e.g., Kuriyama et al. 2020) to make management decisions. More recently, in setting harvest limits for forage fishes, managers have also considered the foraging needs of predators (Marshall et al. 2019; Anstead et al. 2021). These projections typically take stock assessment models, fit to fisheries and biological data, to project biomass values in the near term (1–5 years; e.g., Kuriyama et al. 2020). Forecasts from stock assessment models depend on relatively recent estimates of biological processes like the stock–recruit relationship and growth, with the assumption that these relationships will remain constant for a few years into the future. These projections are not made farther into the future as the stocks are re-assessed regularly as part of the fisheries management program (e.g., every 3 years in the case of Pacific sardine in the US). However, 30–50 years into the future, there will likely be different environmental conditions with corresponding stock status and recruitment regime (e.g., Checkley et al. 2017). Climate-ready fisheries should assess whether current management strategies will be robust to such changes (e.g., Haltuch et al. 2019a).

One proposed solution to the prospect of regime change is to use dynamic reference points in determining stock status for fisheries advice. Indeed, the concept of dynamic reference points was first developed by MacCall et al. (1985) for forage fish. Unlike static reference points that assume stationary stock productivity parameters, dynamic reference points are reflective of current environmental conditions. For example, dynamic estimates of unfished biomass fluctuate over time depending on temporal changes in productivity parameters. In comparing performance of static versus dynamic reference points, recent simulation studies have found that dynamic reference points can be a useful approach to consider the impact of a variable environment in management

advice when the specific mechanisms linking the environment to productivity changes is unknown, although results are species-specific and assume that the productivity change can be correctly attributed to the environment rather than fishing (Berger 2019; O'Leary et al. 2020; Bessell-Browne et al. 2022).

Simulations have also been employed to assess performance of management strategies specific to forage fish. Siple et al. (2019) investigated multiple harvest control rules (HCRs) under various biological and observational uncertainties. For three forage fish-like populations, they tested the performance of rules that used constant exploitation over all stock biomasses, as well as the harvest rule proposed by Pikitch et al. (2012), which triggered reductions in exploitation at a high proportion of unfished biomass. In their investigation, Siple et al. (2019) evaluated performance of the Pikitch rule that closed the fishery at 40% of unfished biomass, as well as a rule with a more gradual decline in exploitation with a fishery closure at 10% of unfished biomass. They found a tradeoff among HCRs between rules that sought to stabilize catch at low stock biomasses and those that maintained stock biomass high enough to avoid fishery closure. This study has improved understanding of best practices in managing highly variable forage fish stocks. However, the robustness of such management strategies to the effects of climate change on these populations must be considered.

Pacific sardine (Sardinops sagax) have been a leading example of the integration of environmental indicators into fisheries management decisions in the United States. In the California Current, their productivity has been linked to oceanographic conditions like curl-driven upwelling (Rykaczewski and Checkley 2008), the Pacific decadal oscillation (PDO; Zwolinski and Demer 2012), and sea surface temperature (SST; Lindegren and Checkley 2013). For over two decades, the northern subpopulation of Pacific sardine has been managed with harvest levels determined with respect to the SST in the southern portion of the California Current ecosystem (PFMC 1998). The current harvest control rule adjusts fishing effort for the advice year based on spring SST measured by the California Cooperative Oceanic Fisheries Investigations (Cal-COFI) program in the 3 years preceding the stock assessment. In addition, Zwolinski and Demer (2012, 2014) have demonstrated a potential relationship between PDO in the months preceding and throughout sardine spawning, with eras of recruitment failure coinciding with the colder phase of a 60-year cycle in PDO. Yet debate continues as to the mechanistic link between these environmental indices and northern Pacific sardine stock recruitment because these relationships between temperature, PDO, and recruitment have recently broken down (McClatchie et al. 2010; Zwolinski and Demer 2019; Muhling et al. 2020). Recent work using a process-based sardine age-structured model shows that the recent collapse in Pacific sardine biomass was likely due to a decline in food availability rather than shifts in temperature (Koenigstein et al. 2022), though the interaction between these drivers is complex and requires further investigation. We must, therefore, consider the vulnerability of management decisions to uncertainty in the assumed SST–sardine relationship.

Fig. 1. Conceptual figure of one iteration of the sardine management strategy evaluation (MSE) showing the operating model (OM) and estimation model (EM) processes. The OM simulates biomass in each year y as a function of recruitment (R_y) and fishing by the Mexican–Californian (MexCal) and Pacific Northwest (PNW) fleets in semesters 1 (July–December) and 2 (January–June). In semester 1, an acoustic-trawl survey index (CCES index) is generated. Fleet data, the CCES index, and size compositions from the survey and fleets from both semesters are sampled with error (dotted arrows) and input into the Stock Synthesis 3 (SS3) EM, which estimates biomass up to year $y - 1$ and a 1-year forecast (year y). Forecast biomass (with assessment error) is used to set total allowable catch (TAC) for year y using an HCR. This TAC is implemented without error and sets the year y catch used in the OM for the following loop of the MSE simulation.
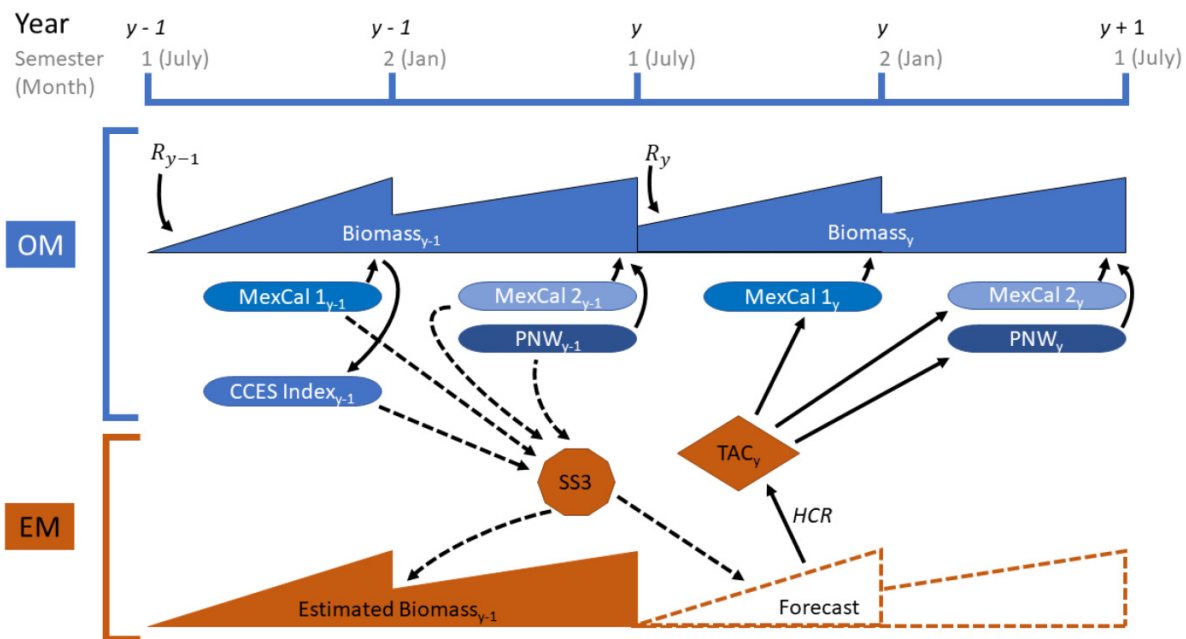
Management strategy evaluation (MSE) provides a method of addressing the uncertainty in environmental stock dynamic linkages by testing the performance of decision rules under a range of system dynamics (Punt et al. 2016a). In MSE, natural processes are simulated in an operating model (OM) that assumes a particular system structure and function, the states of which can then be sampled and assessed with an estimation model (EM). Simulated advice is generated given the sampled data and EM output, and a simulated management action feeds back into the OM to impact the system. This MSE loop (Fig. 1) is iterated and performance of each management strategy is then compared using output from the simulation. An MSE analysis that evaluated performance of alternative management rules for Pacific sardine over a range of stock dynamics was used to select the current northern stock harvest control rule (PFMC 2013; Hurtado-Ferro and Punt 2014). With the advance of climate change, the historical recruitment relationships between the environment and sardine underlying the past MSE analysis may not continue to hold. Because forage fish population dynamics are sensitive to changes in demographic processes, we must assess whether the current SST-based harvest control rule, or any rule, is robust to climate-driven changes in sardine recruitment (ICES 2013). Here too, MSE provides a method in which to test the robustness of these harvest control rules under potential future climate-driven uncertainty (Siple et al. 2021).

We assess management performance of current and alternative harvest control rules to climate-driven recruitment using an MSE of the northern sardine subpopulation. As the response of sardine recruitment to climate change is uncertain, we use multiple scenarios of future recruitment. In addition to the current harvest control rule for Pacific sardine, our analysis also considers rules proposed or applied to forage fish stocks with the intention of maintaining their stock at levels that support fisheries and marine predators (Pikitch et al. 2012). As our analysis includes a simulated stock assessment, it also enables quantification of the efficacy and efficiency of statistical stock assessments for forage fishes. We conclude with a discussion of the implications of single-species management of sardine and other forage stocks in a changing climate, and the importance of monitoring indicators of recruitment of these ecologically integral species.

Methods

The MSE was conducted using the SSMSE package (Doering and Vaughan 2022) in R v4.0.2 (R Project Team 2022). SSMSE uses Stock Synthesis 3 (Methot and Wetzel 2013) to model population dynamics within the MSE loop (Fig. 1). The MSE evaluated the performance of nine HCRs after 50 simulated years under six recruitment scenarios, as described below. Each combination of HCR and recruitment scenario was simulated 500 times to account for process error in recruitment and observation error.

Operating model

The OM has a similar configuration to the 2020 benchmark stock assessment for Pacific sardine (Kuriyama et al. 2020) developed in Stock Synthesis 3.30 (Methot and Wetzel 2013). The OM had two semesters coinciding with the assumed birthdate of sardine on 1 July. Semester 1 (S1) spanned July–December and semester 2 (S2) spanned January–June of the following calendar year (Fig. 1). There were three fishing fleets, representing vessels that fish in waters off Mexico and southern California (MexCal) during S1, another fleet in the same region for S2, and a third fleet that fishes off the coast of Oregon and Washington in S2 (Pacific Northwest). The two MexCal fleets are used to account for differences in age composition between the two semesters, with younger fish caught in S1 and older fish caught in S2. The three fishery-independent data sources all derive from the Southwest Fisheries Science Center's California Current Ecosystem Survey, which targets coastal pelagic species using a combined acoustic-trawl method. They were (1) an acoustic-trawl survey abundance index (CCES index, 2005–2019; e.g., Stierhoff et al. 2020; Renfree et al. 2023), (2) daily egg production (DEPM, 2003–2014; e.g., Dorval et al. 2014), and (3) total egg production (TEP, 2001–2014; e.g., Dorval et al. 2014). Marginal age and length compositions were additional biological data sources for the three fishing fleets and the acoustic-trawl survey.

The OM differed from the benchmark assessment in that it had a longer modeled time period, included DEPM and TEP as additional indices of abundance, and estimated time-invariant age-based selectivity and time-invariant growth from marginal age and length compositions rather than using empirical weight-at-age. The OM modeled time period was 2001–2019, whereas the benchmark spanned 2005–2019. This longer time period was possible due to the inclusion of the DEPM and TEP indices. Both egg production indices represented a measure of spawning stock biomass (SSB) and were designed to survey small pelagic fish like sardine (Lo et al. 2005; Wolf and Smith 1985). The time-invariant age-based selectivity can be thought of as fish availability to fishing or survey gear. Growth estimation followed the Stock Synthesis 3 parameterization of a von Bertalanffy growth curve (Methot and Wetzel 2013).

The OM is able to recreate observations of the 2001–2019 northern Pacific sardine stock and its fleets; we view this as necessary if we are to use it as simulated "truth" in the MSE. In the OM, some influential scaling parameters (steepness, mortality, and catchability) were assumed to be fixed, while the growth and selectivity parameters were estimated, conditioned on data from 2001 to 2019. Catchability parameters for the acoustic-trawl, TEP, and DEPM surveys were assumed to be 1, 0.55, and 0.16, respectively. These parameter values were estimated in previous versions of the sardine benchmark assessments. Natural mortality was assumed to be 0.585, and steepness assumed to be 0.6 (values also used in previous assessments). Length-based selectivity was assumed to be asymptotic and estimated from data from 2001 to 2019. The age-based selectivity was estimated with the nonparametric form (option 17 in SS3), which estimates a selectivity parameter for each age rather than imposing a particular

form. Even without time-varying growth and selectivity, the OM could reasonably represent historical biomass estimates (Figs. S1 and S2). During the forward simulation from 2020 to 2070, all OM model parameters except for annual recruitment deviates were kept constant to the values estimated during the 2001–2019 conditioning period (Table S1). Future recruitment deviates were generated differently for each of the six recruitment scenarios to account for uncertainty in future recruitment (see below; Table 1) and input into the OM as a driver of the 50-year simulation.

Recruitment scenarios

We assessed robustness of management strategies to one source of uncertainty: process error in future recruitment (i.e., random recruitment variation, modeled as deviations from a mean recruitment model). Future recruitment deviations were generated differently for each of six recruitment scenarios to account for uncertainty in future recruitment (see below; Table 1, Fig. 2) and input into the OM as a driver of the 50-year simulation. Three of these scenarios (Future SST, Future PDO, and mechanistic, age-structured sardine population dynamic (MICE)) integrated output from climate projections to drive future recruitment deviations in the MSE and are considered the *climate change effect* scenarios. The remaining three recruitment scenarios consider recruitment deviations as shifting between high and low periods with no directional climate change effect imposed. These are considered the *no climate change effect* scenarios.

Each of the six recruitment scenarios (Table 1) is forced with log-normal recruitment deviations around a common Beverton–Holt stock–recruit relationship defined in the OM:

$$(1) \quad \widehat{R}_y = \frac{4hR_0 \text{SB}_y}{\text{SB}_y(1-h) + \text{SB}_y(5h-1)} e^{-0.5b_y\sigma_R^2 + \tilde{R}_y}$$

The expected recruitment in year y ($\hat{R}_y$) is a function of spawning biomass in year y (SB_y), steepness ($h = 0.6$), recruitment produced from an unfished stock (R_0), recruitment variance ($\sigma_R^2 = 1.25$), a bias adjustment fraction (b_y), and a normally distributed recruitment deviation ($\tilde{R}_y$) (Methot and Wetzel 2013, Appendix A). To account for process error in each recruitment scenario and sampling error, 500 random replicates were evaluated for each scenario. These random draws of recruitment deviations were kept consistent across HCRs.

Two recruitment scenarios without climate change effects used built-in SSMSE options for projecting log-normal recruitment deviations. The autocorrelated random recruitment scenario sampled future recruitment deviations from a normal distribution of zero mean and standard deviation (SD), σ_R, of 1.25 as in the conditioning period with annual autocorrelation of $\rho_R = 0.678$. This level of autocorrelation was that of recruitment deviations from the conditioning period. The second scenario was developed to represent a shift from the current low recruitment regime to a high recruitment period after 25 years. In the first low recruitment period, recruitment deviations were sampled from the same normal distribution as the first scenario but without autocorrelation. Then, a bias adjustment was applied to the mean of the recruitment deviations starting in projection year 2045 to sim-

Table 1. Recruitment scenarios. $\tilde{R}_y$ are the log-normal recruitment deviations for year y in the forward MSE simulation.

Scenario	Description	Formulation	Reference
Autocorrelated recruitment	Random normal recruitment deviations with the same mean and standard deviation used in the conditioning period and autocorrelation at $\rho_R = 0.678$	$\tilde{R}_y = \rho_R \times \tilde{R}_{y-1} + \widehat{R}_y$ $\widehat{R}_y \sim N\left(\mu_{hist} = 0, \frac{\sigma_{hist}}{\sqrt{1/(1-\rho_R^2)}}\right)$ $\rho_R = 0.678$, $\sigma_{hist} = 1.25$	Methot and Wetzel (2013) See eq. in Maunder and Thorson (2019)
Regime recruitment (low to high)	Random normal recruitment deviations with the same mean and standard deviation used in the conditioning period for the first 25 years of the simulation, then switching to deviations with a mean = 1 thereafter	$\tilde{R}_y = \tilde{R}_{y-1} + \widehat{R}_y$ $\widehat{R}_y \sim N(\mu_y, \sigma_{hist})$ $\mu_y = \begin{cases} \mu_{hist} = 0, & y < 2045 \\ \mu_{high} = 1, & y \geq 2045 \end{cases}$ $\sigma_{hist} = 1.25$	Kuriyama et al. in review
Cyclic PDO	Recruitment deviations are calculated as random normal deviates around the mean PDO index derived from fitting a 60-year cycle to historical PDO data	$\tilde{R}_y = \eta(\widehat{R}_y \times 0.44 + \varepsilon_t \times 0.56)$ $\widehat{R}_y = \sin(2\pi t/60)$ $\eta = \sigma_{OM}/\sigma_{ROMS\ PDO} = 1.25/0.714$ $\varepsilon_t \sim N(0, \sigma_{OM})$	Zwolinski and Demer (2019, 2014)
Future PDO	As in the cyclic PDO index, but the combined mean PDO index is derived from bias adjusted ROMS climate projections.	$\tilde{R}_y = \eta(\widehat{R}_y \times 0.44 + \varepsilon_y \times 0.56)$ $\widehat{R}_y = 0.7815x_{ROMS\ PDO,\ y}$ $\eta = \sigma_{OM}/\sigma_{PDO} = 1.25/0.763$ $\varepsilon_y \sim N(0, \sigma_{OM})$	Zwolinski and Demer (2019, 2014)
Future SST	Recruitment deviations are calculated as random normal around the difference between annual CalCOFI region SST regression term and the regression term using the average historical SST. Annual CalCOFI SST is derived from bias adjusted ROMS climate projections	$\tilde{R}_y = \eta(\widehat{R}_y \times 0.55 + \varepsilon_y \times 0.45)$ $\widehat{R}_y = 1.28x_{SST,\ y} - 1.28x_{\overline{SST}}$ $\eta = \sigma_{OM}/\sigma_{SST} = 1.25/0.699$ $\varepsilon_y \sim N(0, \sigma_{OM})$	PFMC 2013, Appendix H
MICE ensemble recruitment	Recruitment deviations are residuals from a Beverton–Holt stock–recruit relationship fit to abundance-at-age output from a mechanistic sardine population dynamics model averaged over nine model structures and three climate projections. Fit residuals are scaled to match the variation of historical deviations in the OM model	$\tilde{R}_y = \eta(\widehat{R}_y \times 0.7 + \varepsilon_y \times 0.3)$ $\widehat{R}_y = R_{MICE,\ t} - aSB_{y-1}/(b + SB_{y-1})$ $a = 2.7 \times 10^9$ $b = 1.3 \times 10^5$ $\eta = \sigma_{OM}/\sigma_{MICE} = 1.25/0.421$ $\varepsilon_y \sim N(0, \sigma_{OM})$	Koenigstein et al. (2022)

Note: Scenarios in bold are those that integrate climate change effects. MSE, management strategy evaluation; PDO, Pacific decadal oscillation; SST, sea surface temperature; CalCOFI, California Cooperative Oceanic Fisheries Investigations; OM, operating model; ROMS, regional ocean modeling system; model of intermediate complexity for ecosystem dynamics (MICE), mechanistic, age-structured sardine population dynamic.

ulate an upward shift in mean recruitment. This bias adjustment reflects the difference in the mean of early (1981–2000) and late (2001–2019) recruitment deviations estimated in the original conditioning of the OM model, characterizing eras of high recruitment and stock biomass, followed by recruitment failure and fishery collapse. In all recruitment scenarios, recruitment deviations were generated independently for each scenario replicate, but were applied similarly across HCRs within recruitment scenarios to ensure comparability.

The remaining recruitment scenarios assume that some of the variability in recruitment deviations can be explained by an environmental covariate (CV) according to the equation below:

$$(2) \qquad \tilde{R}_y = r^2 * e^{\beta V} + (1 - r^2) * e^{\varepsilon_y}$$

where β is the effect of the environmental covariate V on recruitment via the larval/juvenile fish mortality rate (Maunder and Thorson 2019). The r^2 determines what proportion of

the yearly recruitment deviations ($\tilde{R}_y$) is generated by the environmental CV and what proportion is explained by a random error (ε_y), where ε_y is drawn from a random normal distribution with mean 0 and SD of 1.25. In the SST and PDO scenarios (see below), this proportion was assumed to be the r^2 from the study in which the relationship was estimated, and the deviance explained by the MICE ensemble (see below) was assumed to be $r^2 = 0.7$, following Siple et al. (2019). To ensure continuity of recruitment variance, the SD of the total recruitment deviations (environmentally driven effect + random) in environmentally driven scenarios were scaled to the historical SD ($\sigma_R = 1.25$).

The third no climate change effect scenario assumed that recruitment deviations around the mean stock–recruit relationship were a function of the PDO index described by Zwolinski and Demer (2019). This scenario fit a 60-year cycle to historical PDO data (https://www.integratedecosystemass essment.noaa.gov/index.php/regions/california-current/cali fornia-current-iea-indicators) using a sine link function as

Fig. 2. (A) Example time series of age 1+ biomass and (B) recruitment deviations generated by the operating model for each recruitment scenario. Median (black line, panel A), individual iteration time series (gray lines), and three randomly sampled time series with matching colors are shown. The biomass cutoff threshold value relevant for management (flat red line, panel A) is shown at 150 000 mt. The break between the model conditioning and projection periods is also shown at 2019 (vertical dashed lines).
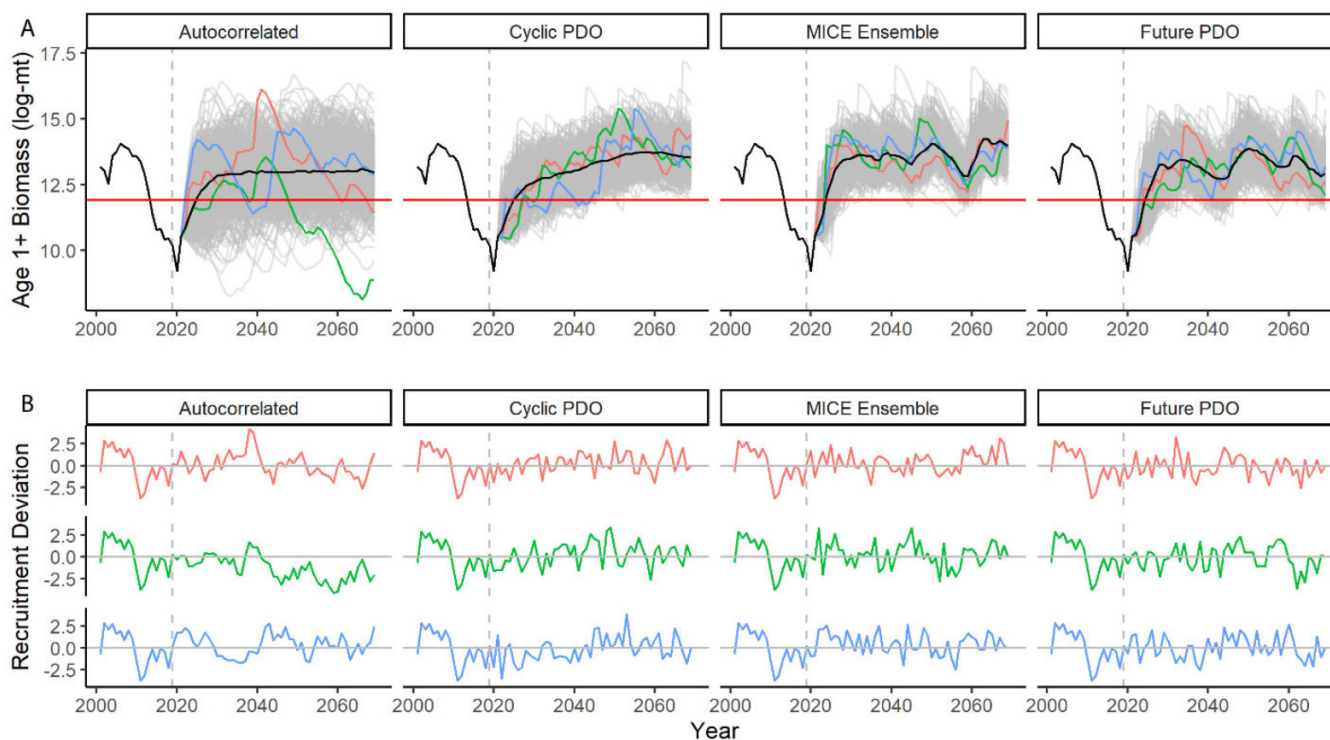
the CV effect on the deviations (Zwolinski and Demer 2014). The corresponding recruitment scenario incorporating climate change effects on Future PDO was calculated using the projected PDO monthly index time series averaged over three earth system models (Pozo Buil et al. 2021) and then bias adjusted, so the mean of the earth system model ensemble historical period (i.e., 1976–2020) was equal to that used in the fitting of the PDO–recruitment relationship. The fifth recruitment scenario (Future SST) was calculated using a similar approach but used the relationship between recruitment and annual SST in the region of the CalCOFI hydrographic and plankton survey (Hurtado-Ferro and Punt 2014). This scenario used the SST–recruitment function defined in the Pacific Fishery Management Council (PFMC) documentation to identify the environmental HCR currently used to manage the stock (PFMC 2022). The CV effect on the deviations in this scenario was calculated as the difference between the SST effect in year t and the mean SST effect over the years used to fit the original environmentally informed stock recruitment relationship and temperatures projected from the same global climate models as in the Future PDO scenario.

The sixth and final recruitment scenario derived recruitment deviations from an ensemble of MICE models (Koenigstein et al. 2022). This ensemble has finer resolution of early life stage dynamics and used mechanistic relationships with environmental drivers to drive variation in egg production and larval survival. These mechanistic

models were calibrated to provide similar biomass trends over the conditioning period as the Stock Synthesis model on which the OM for this study was based (Koenigstein et al. 2022). However, models in the MICE ensemble do not have a stock–recruitment relationship as used in the OM model formulation. Recruitment was instead a result of explicitly resolved early life stage survival processes driven by temperature, food availability, ocean transport, and food-driven egg production, as well as density-dependence feedbacks (Koenigstein et al. 2022). Therefore, we fit a separate Beverton–Holt stock–recruit relationship using the MICE ensemble mean abundance of late-stage age 0 fish as the response variable (recruits) and SSB calculated as the sum product of the MICE ensemble mean abundance of ages 1 to 8 fish, the mean weight-at-age, and the mean maturity-at-age keys from the sardine stock assessment:

$$(3) \qquad \mathrm{SSB}_t = \sum_{a=1}^{8} N_{a,t} w_a m_a$$

where $N_{a,t}$ was the abundance at age a at time t, w_a was mean weight at age a, and m_a was mean proportion mature at age a. The recruitment deviations in this scenario were calculated as the difference between the MICE ensemble recruit abundance at time t and the maximum likelihood estimate of expected recruitment from the fitted stock–recruit relationship.

Environmental CVs are required for the Future SST, Future PDO, and MICE ensemble scenarios. These were derived from a regional ocean modeling system (ROMS) for the California Current ecosystem that provided downscaled projections from three earth system models using the Intergovernmental Panel for Climate Change emissions scenario RCP 8.5: the Geophysical Fluid Dynamics Laboratory (ESM2M), Hadley (HadGEM2-ES), and Institut Pierre Simon Laplace (CM5A-MR) climate models (Pozo Buil et al. 2021). These downscaled ROMS-projected time series included SST within the CalCOFI survey area for the Future SST scenario and SST and food availability (nanophytoplankton and microzooplankton) over early life stage habitat, and food availability (diatoms, mesozooplankton and krill) over adult habitat for the MICE ensemble scenario (see Koenigstein et al. 2022). Projections for the Future PDO were computed directly from the three earth system models. The projected time series were model averaged annually and used as CVs in our recruitment scenarios.

Estimation model

Integrating an EM within the MSE loop (Fig. 1) allows for an assessment of HCR performance considering observation and assessment error, in addition to recruitment uncertainty. The EM structure was similar to the OM model, but as in the current sardine assessment (Kuriyama et al. 2020), the EM was fit to fishery and CCES index data starting in 2005 rather than from the 2001 OM start date. Unlike the OM, which fixed all parameters during the forward MSE projection period, the EM estimated growth and recruitment parameters given data with error sampled from the OM. To reduce convergence issues, selectivity was not estimated and assumed at values equal to the parameters in the OM. At each time step of the simulation, catch, CCES biomass index, and size composition data were sampled with error from the OM (based on the current 1-year stock assessment frequency for Pacific sardine) and input into the EM. Data for input into the EM were generated within SSMSE using Stock Synthesis bootstrap capabilities that generate new datasets of random observations using the same variance properties (standard error of fleet specific catch, standard error of the CCES biomass index, and effective sample size of the size composition data) and error structure (log-normal for catch and CPUE, multinomial for the size composition data) assumed during the OM conditioning phase. The composition samples had assumed sample sizes approximately equal to their mean during the conditioning period, while the CCES index and catches were sampled with CVs of 0.25 and 0.05, respectively. We found that using this observation error generated reasonable assessment errors while minimizing convergence issues (see *Estimation Model Fit*). Convergence was defined as a maximum gradient of the objective function less than 0.01. Because of the nature of the SSMSE simulation software, non-converged assessments still informed management within the MSE loop, but all assessment error statistics were calculated with assessment output from converged EM models only (see *Performance Metrics* below). As under current management, the EM (i.e., simulated assessment) was used to forecast age

1+ biomass at the start of the upcoming fishing seasons to set the total allowable catch (TAC) as determined by one of nine harvest control rules (Fig. 3). Considering the 50-year simulation period and the 1-year stock assessment frequency, this resulted in 50 rounds of EM fitting for each iteration and HCR.

The EM successfully converged in 94.5% of 700 000 simulated assessments (one assessment per year for 50 years × 500 replicates × 7 EM-based HCRs × 4 recruitment reference scenarios). Relative assessment error for year y was calculated as the percent difference in age 1+ biomass estimated by the EM relative to the age 1+ biomass projected by the OM:

$$\mathrm{RE}_y = \frac{\widehat{B}_y^{\mathrm{EM}} - B_y^{\mathrm{OM}}}{B_y^{\mathrm{OM}}} \times 100$$

For any single EM fit, the terminal (final) year of the assessment tended to underestimate age 1+ biomass relative to the OM. Since there is no assessment under the index-based HCR, the relative "assessment" error for that rule was computed as the difference between the stock biomass as estimated by the CCES index and that from the OM:

$$\mathrm{RE}_y = \frac{B_{y-1}^{\mathrm{Index}} - B_y^{\mathrm{OM}}}{B_y^{\mathrm{OM}}} \times 100$$

Note that the latest available summer acoustic-trawl survey occurs 1 year before the harvest guideline is implemented, so the CCES index-based biomass is compared to the OM biomass in the following year. See *Estimation Model Fit* and *Harvest Control Rule Performance* in the Results section for further discussion of the EM assessment error.

Harvest control rules

Deroba and Bence (2008) summarize features of harvest control rules, which we generalize here in Fig. 4. In its simplest form, an HCR defines a precautionary target exploitation rate (E_{target}) that is constant over all stock biomass levels. Alternatively, E_{target} can vary through time, for example, based on an environmental indicator as in the sardine SST-based HCR implemented by the PFMC (PFMC 2022). Furthermore, at low biomasses, exploitation can be reduced to 0 to preserve spawning potential at the cost of annual catch. The biomass reference point at which exploitation is set to 0 (B_{limit}) determines when the fishery closes, as well as the slope of the HCR between exploitation rates of 0 and E_{target}. As B_{limit} moves closer to the biomass at which E_{target} is triggered (B_{trigger}), the slope of the HCR increases along with the proportion of preserved biomass and variability in catch. The extreme case where $B_{\mathrm{limit}} = B_{\mathrm{trigger}}$, termed a threshold or "bang-bang" HCR (sensu Deroba and Bence 2008), results in high catch variability as the fishery closes completely with slight variation in stock biomass. At the right of Fig. 4, the implementation of a maximum catch cap reduces exploitation above some bonanza stock biomass (B_{bonanza}, i.e., a level of exceptionally high biomass; Siple et al. 2019) and reduces variability from high catches. A maximum catch was implemented in all HCRs tested in this study.

Fig. 3. Example time series of age 1+ biomass (A) and total catch (C) for each of the HCRs, recruitment deviations (B), and relative error of the terminal estimate (D) for an iteration of the MICE recruitment scenario. This example depicts modeled variation in biomass (and catch) under the nine HCRs, with stock declines (A) dependent on recruitment variation (B) and catch (C). Note the different *y*-axis limits in A and C. Age 1+ biomass is plotted alongside the 150 000 cutoff and 50 000 collapse thresholds (red horizontal lines) in panel A. Years of poor recruitment (deviations <-1.25) are indicated with black points in panel B. The 200 000 mt MAXCAT catch limit is shown in grey in panel C. Relative error in terminal year biomass (solid line) and CCES index data provided to the estimation model (open squares) from the PFMCFSST HCR application to the same iteration are compared in panel D. All lines in A and C overlay in the historical period.
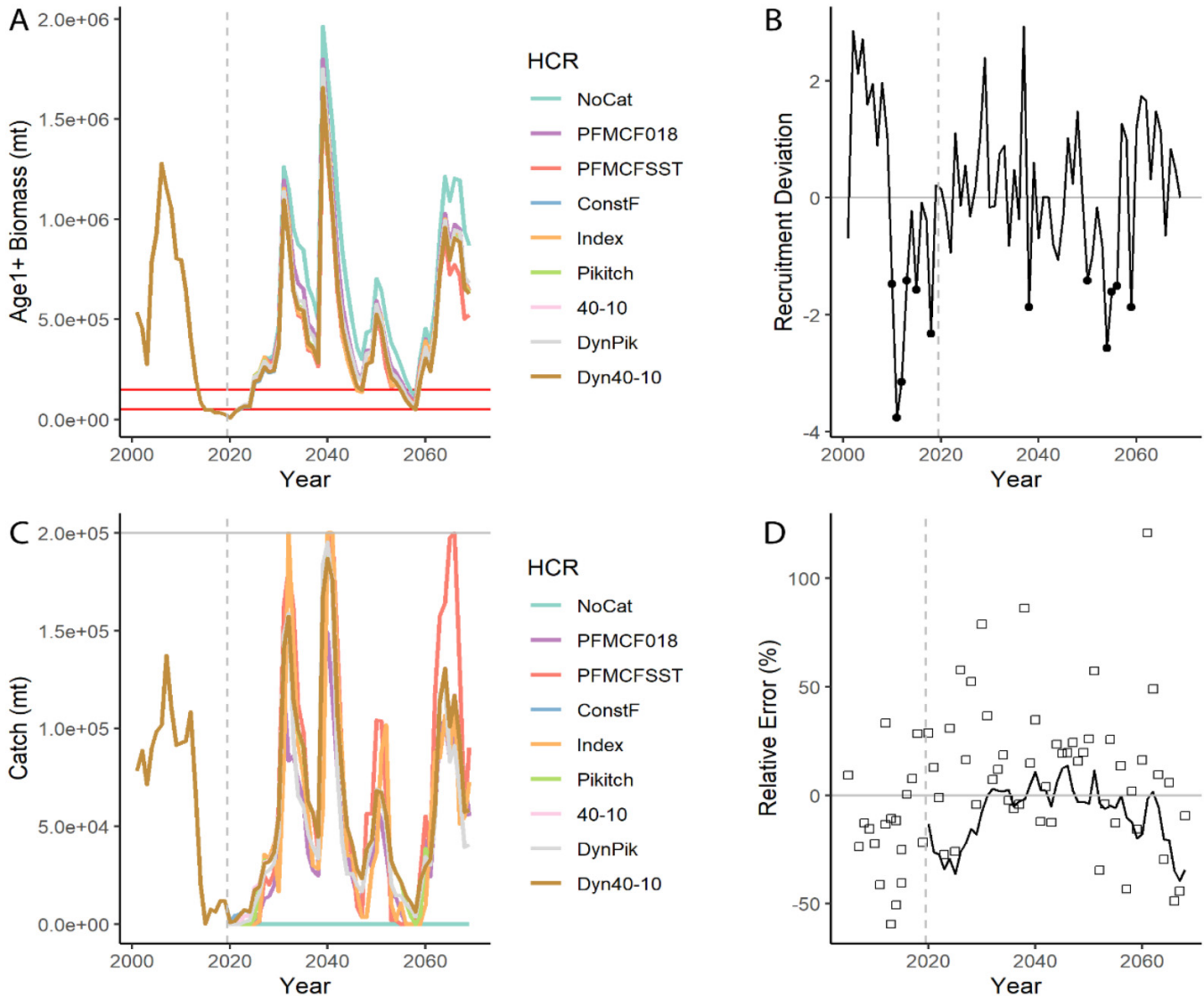
Nine harvest control rules (Table 2, Fig. 5) were tested in each recruitment scenario. Since sardine biomass dynamics are highly variable even with no fishing, the first HCR enacted zero catch over the projection period (NoCat). The next two HCRs (PFMCF018 and PFMCFSST) tested the current rule used in the fishery, which defines a threshold rule with zero catch under a precautionary age 1+ stock biomass cutoff ($B_{Cutoff} = 150\,000$ mt), and catch proportional to age 1+ stock biomass (B) at higher biomass according to an annual exploitation rate, E_y, until a maximum catch limit (MAXCAT) of 200 000 mt (PFMC 2022):

(4) $\text{Total Catch}_y = \min\left((B_y - B_{Cutoff}) * E_y * \text{Dist}, \text{MAXCAT}\right)$

where E_y is the annual exploitation rate, Dist is the proportion of the sardine stock distribution in US waters (assumed to be 0.87), and min() indicates that when MAXCAT $< (B_y - B_{Cutoff}) * E_y * $ Dist, the MAXCAT is provided as the total catch advice. This catch advice applies to the year y following the year of the assessment (Fig. 1), thus B_y is the biomass forecast by the assessment for the beginning of the upcoming fishing year (PFMC 2022). First, we tested a version of this HCR with a stationary exploitation rate set to maximum sustainable yield ($E_{MSY} = 0.18$) as estimated by Hill et al. (2011, Appendix 4). The second version of this rule emulated the HCR currently applied to the northern sardine stock and modified E_y as an approximately linear function of SST as defined in

Fig. 4. Conceptual guide mapping performance metrics to harvest control rule shape following Deroba and Bence (2008). A target exploitation rate (E_{target}) chosen below some limit rate (E_{limit}) ensures precaution. A constant E_{target} over stock biomasses encourages low catch variability, while changes in this rate over time increase catch variability. Reducing the exploitation rate below some threshold or "trigger" stock biomass ($B_{trigger}$), and potentially closing the fishery below a biomass limit (B_{limit}) trades off consistency in catch to preserve spawning potential. Increasing the level of $B_{trigger}$ or B_{limit} leads to more catch variability and more frequent fishery closures. Implementing a maximum cap on catches reduces average catch, variation in catches, and reduces the exploitation rate during bonanzas (periods of high stock biomass).
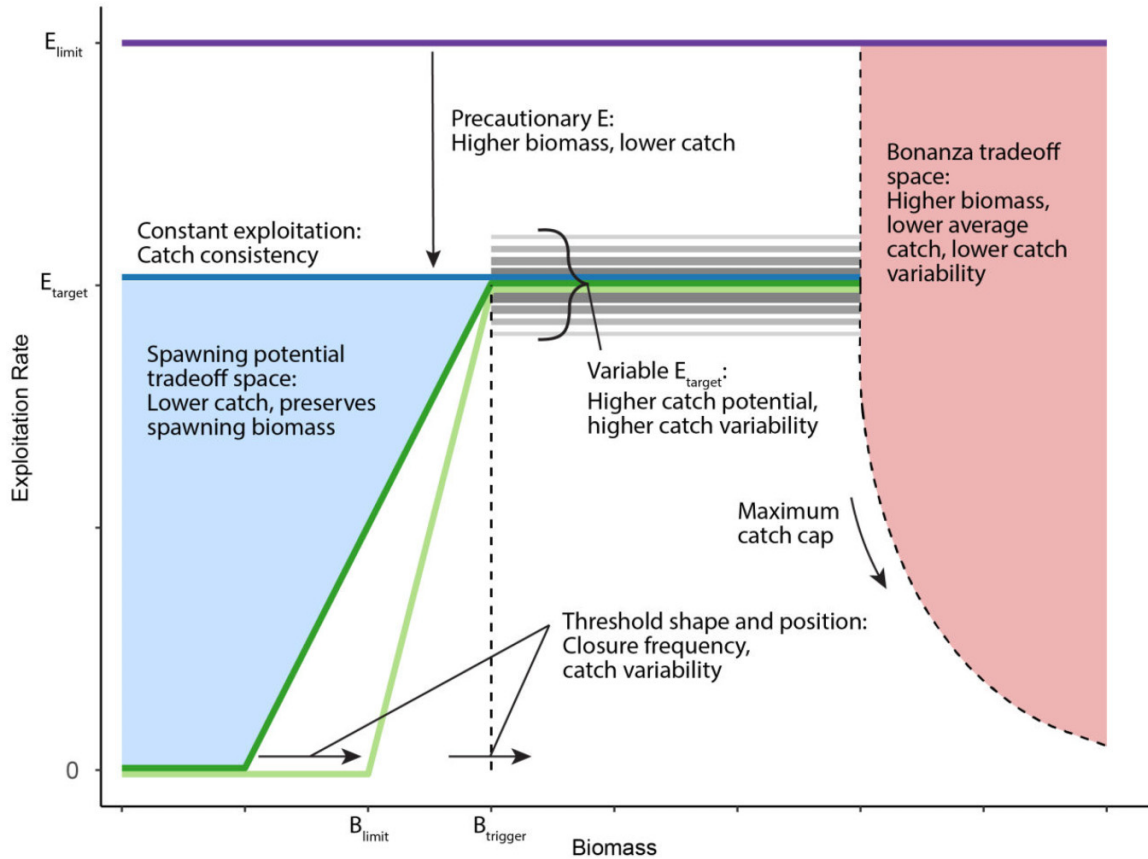
Table 2. Description of harvest control rules.

| HCR code	HCR	Description	Reference
NoCat	No Catch	Control run with zero catches	
PFMCF018	Current HCR but with fixed E_{MSY}	Broken stick with current CUTOFF and MAXCAT and exploitation rate set to 0.18	Hill et al. (2011), Appendix 4
PFMCFSST	CalCOFI SST E_{MSY} (current)	Exploitation rate is modified as a function of the 3-year mean of CalCOFI sea surface temperature	PFMC (2022)
ConstF	Constant exploitation	A constant $E = 0.18$ is applied throughout the projection period, but MAXCAT still applied	
Index	Index-based	Threshold rule as in PFMCF018 applied to simulated CCES index in the assessment year ($y - 1$)	
Pikitch	Pikitch forage rule with E_{target} set to 0.18	Broken stick with B_{limit} of $0.4B_0$, $B_{trigger}$ of $0.8B_0$, and $E_{target} = 0.18$	Pikitch et al. (2012)
40-10	40-10 rule	Broken stick with B_{limit} of $0.1B_0$, $B_{trigger}$ of $0.4B_0$, and $E_{target} = 0.18$	PFMC (2016)
DynPik	Dynamic Pikitch	Same as Pikitch rule but with dynamic B_0	Berger (2019)
Dyn40-10	Dynamic 40-10 rule	Same as 40-10 rule but with dynamic B_0	Berger (2019)

the PFMC's Coastal Pelagic Species Fishery Management Plan (PFMC 2022):

(5) $\quad E_{SST} = 0.248649805\,T^2 - 8.190043975\,T + 67.45583262$

where T is the 3-year annual mean SST over the CalCOFI survey region. This temperature-based HCR functioned similarly to the one currently applied to the northern stock by the PFMC. These HCRs were compared to a fourth HCR (Con-

Fig. 5. Example of the HCR forms used for the management strategy evaluation in this study. All HCRs (except the ConstF rule) increase from an exploitation rate of 0 at low biomass to an E_{target} defined by each rule. The PFMCF018, ConstF, Pikitch, and 40-10 rules have an $E_{\text{target}} = 0.18$. The PFMCFSST rule ranges from $E_{\text{target}} = 0.05$ at low temperatures to $E_{\text{target}} = 0.20$ at higher temperatures. The B_{limit} and B_{trigger} values used in the Pikitch and 40-10 rules are calculated as a proportion of the unfished biomass (B_0, vertical grey dotted lines). In the dynamic versions of this rule, the estimate of B_0 may vary throughout the simulation. Note that horizontal portions of HCR lines are slightly shifted here to improve visualization of each rule.
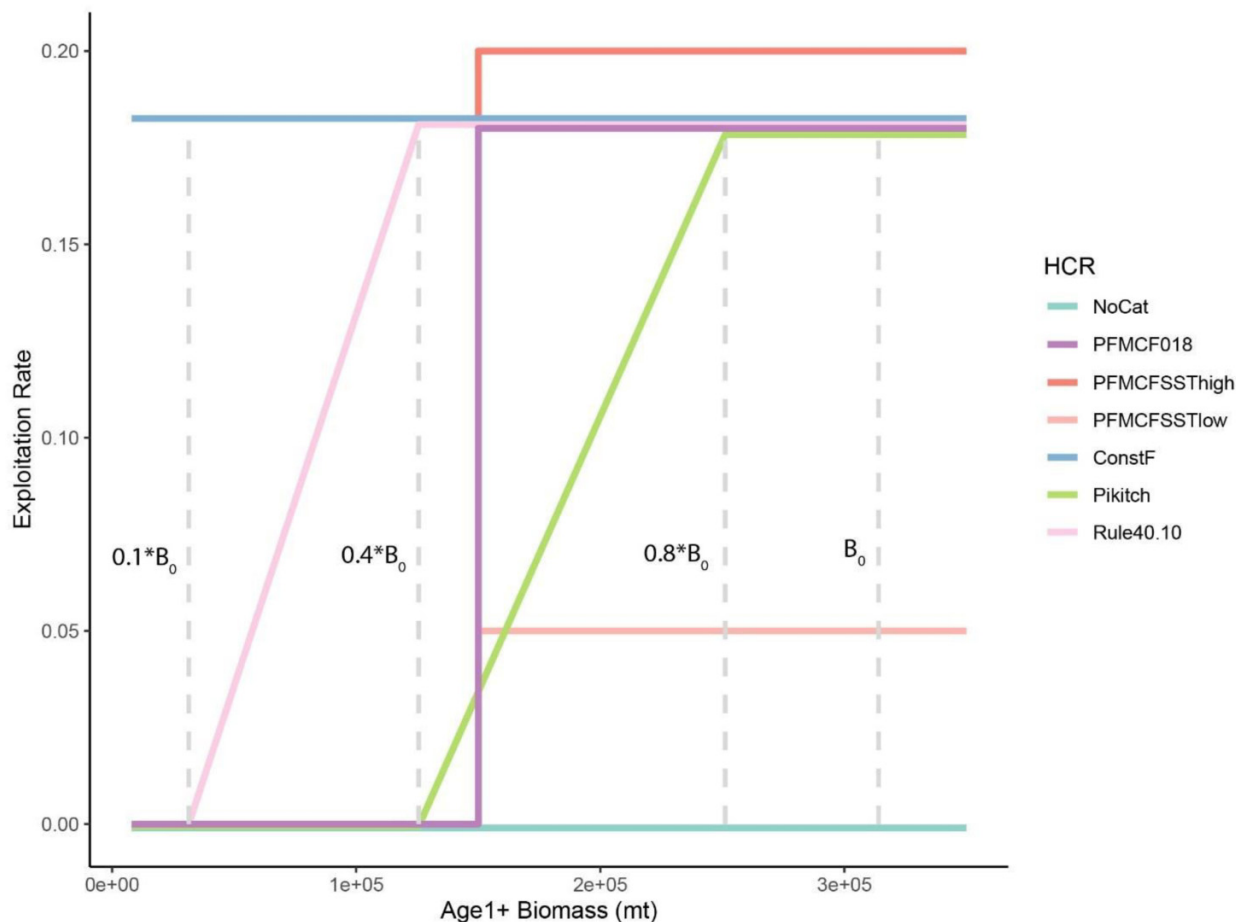
stF), which was the same as the PFMC E_{MSY} HCR (PFMCF018) but without the cutoff at low biomass. Thus, it implemented a constant exploitation rate for maximum sustainable yield ($E_{\text{MSY}} = 0.18$) up to the MAXCAT catch limit. A fifth HCR (Index) applied eq. 4 with $E_{\text{MSY}} = 0.18$ to an index value of B_{y-1} estimated from the summer CCES index in the assessment year ($y-1$) rather than the Stock Synthesis model-based biomass forecast for the upcoming fishing year y. For this rule, catchability was assumed to be 1, assuming that the CCES index is an absolute index of abundance.

The next set of HCRs (rules 6–9) took the form of broken stick rules that were developed in the fisheries management literature to apply more generally to other forage fish and groundfish stocks. The sixth rule (Pikitch) was derived from Pikitch et al.'s (2012) simulation study and tests a rule with $E_y = E_{\text{MSY}}$ when SSB_y is $\geq 0.8 * SSB_0$ up to the MAXCAT limit, where SSB_0 is the estimated unfished spawning stock biomass. E_y is 0 if SSB falls below $SSB_{\text{limit}} = 0.4 \times SSB_0$. At intermediate levels of SSB_y, the Pikitch HCR applied a decreasing exploitation rate:

$$(6) \quad \text{Total Catch}_y = \begin{cases} \text{MAXCAT}, & 0.18 B_y * \text{Dist} > \text{MAXCAT} \\ 0.18 B_y * \text{Dist}, & SSB_{y-1} > 0.8 SSB_0 \\ \dfrac{0.18 B_y * (SSB_{y-1} - 0.4 SSB_0) * \text{Dist}}{0.8 SSB_0 - 0.4 SSB_0}, & 0.4 SSB_0 < SSB_{y-1} < 0.8 SSB_0 \\ 0, & SSB_{y-1} < 0.4 SSB_0 \end{cases}$$

The seventh HCR (40-10) followed the 40-10 rule used in management of groundfish off the US West Coast (PFMC 2016). It was the same as the Pikitch HCR, but applies a biomass limit of $SSB_{limit} = 0.1 * SSB_0$ and an upper threshold biomass corresponding to $0.4 * SSB_0$. The final two HCRs (DynPik and Dyn40-10) applied the Pikitch rule and 40-10 rule with E_{MSY} but used dynamic reference points with respect to SSB_0 (Berger 2019). Dynamic SSB_0 is the unfished biomass that fluctuates through time given changes in productivity, such as recruitment. In the EM, it varies annually and is estimated in Stock Synthesis by running the population trajectory with the exploitation rate set to 0 and all the other parameters kept the same as those estimated with fishing. Here, in contrast to Haltuch et al. (2019a), annual dynamic SSB_0 estimates were not averaged over estimation years. The SSB_0 estimate for the terminal year was compared to terminal year SSB (SSB_{y-1} in eq. 6). These biomass reference points were calculated within the MSE simulation from the EM and applied annually to determine the total catch according to eq. 6.

For all but the no catch and survey index-based HCRs, 1-year forecast age 1+ biomass for the upcoming fishing year from the EM was used in eq. 4 or 6 to derive catch advice as is done in current management of the Pacific sardine subpopulation (PFMC 2022; Fig. 1). In each recruitment scenario–HCR combination, catch advice was implemented without error and allocated to the fisheries based on the mean catch ratio observed among the three fleets from 2006 to 2011. This period was selected because the allocation scheme changed in 2006 from a regional to a seasonal allocation.

Performance metrics

We calculated 11 performance metrics over the 50-year projection period that relate to fishery and conservation objectives (Table 3). To compare relative performance among climate and non-climate change recruitment scenarios, we pooled metrics across scenarios for each of these climate categories. For consistency among HCRs, we use reference points defined in the current sardine stock assessment for calculating performance. Performance metrics related to fishery objectives included median and SD of annual total catches, closure frequency, number of closures, and rebuilding period length. For sardine stock status, we reported the median annual stock biomass for age 1+ fish and older and collapse frequency and severity (Siple et al. 2019). Cutoff frequency also relates to conservation objectives: some of the original motivation for the CUTOFF biomass was to maintain minimum forage availability to predators. To compare relative performance of each HCR with respect to the baseline for each recruitment scenario, we calculated catch and stock biomass metrics relative to the mean value within each recruitment scenario and across all iterations and projection years. Lastly, we reported the EM error rate in the terminal (i.e., final) year of the assessment with respect to two management thresholds. We summarized the proportion of incorrect advice (from the EM) regarding whether the stock size was below the cutoff threshold (age 1+ biomass <150 000 mt) and when it was below the collapse threshold (age 1+ biomass <50 000 mt). We summed instances where the EM estimated the population below the cutoff (collapse) threshold, but the OM biomass was above that threshold (false alarms), and the reverse where the EM estimated higher population biomass, but the OM biomass was below the cutoff (collapse) threshold (misses). Total error was calculated as the sum of false positive (false alarms) and false negative errors (misses) (Piet and Rice 2004).

Results

Simulation dynamics

OM and recruitment scenarios

Simulated northern Pacific sardine stock biomass recovered quickly from its collapsed condition ($B_{2019} = 26\,030 < 50\,000$ mt) at the beginning of the simulation in all recruitment scenarios (Fig. 2 for reference set scenarios, see below for reference set definition). Under a no catch strategy (NoCat), biomass in the majority of iterations in all recruitment scenarios had recovered to levels greater than 150 000 mt by 2025; however, 5% of all iterations had not rebuilt above this threshold by 2032. With autocorrelated recruitment, biomass was above the 150 000 mt cutoff threshold in 76.2% of all projection years (50 years $*$ 500 iterations), below the cutoff but above collapse in 15.8% of projection years, and below the collapse threshold in 8.0% of projection years (Fig. 2A). The cyclic PDO scenario exhibited a more consistent increase in biomass through the projection with a peak in 2056, mirroring the underlying 60-year PDO cycle driving the scenario. Biomass in this scenario was below the collapse threshold in 6.0% of projection years and above the cutoff threshold in 86.0% of projection years. The MICE and Future PDO scenarios had collapsed biomass levels in 5.3% and 6.4% of projection years and biomass above the cutoff threshold in 91.1% and 88.8% of projection years, respectively. Across all scenarios, 2020–2029 had the highest frequency of biomass below collapsed and cutoff thresholds, although the frequency of biomass between 50 000 and 150 000 mt increased slightly in the 2050s for the MICE scenario (0.6% of projection years) and in the 2040s for the Future PDO scenario (2.9% of projection years).

In the autocorrelated recruitment scenario, recruitment deviations were generally within one SD of the mean with a few extreme peaks occurring in each iteration (e.g., Fig. 2B). Recruitment deviations in both PDO scenarios were centered near zero (Future PDO: $\bar{R}_{PDOclim} = 0.007$; cyclic PDO: $\bar{R}_{PDOcycl} = 0.07$). The recruitment deviations in the MICE scenario were positively biased ($\bar{R}_{MICE} = 0.39$), indicative of a climate-driven directional shift in recruitment. The recruitment deviations in the regime and Future SST scenarios were also positively biased ($\bar{R}_{Reg} = 0.50$ and $\bar{R}_{SST} = 1.8$, respectively), though this was expected as these scenarios were designed a priori to evaluate effects of this regime shift on management outcomes. These positively biased recruitment deviations in the regime and Future SST scenarios led to large projected biomasses throughout the projection period (Fig. S3). Biomass in these two scenarios exhibited two phases,

Can. J. Fish. Aquat. Sci. **00**: 1–23 (2023) | dx.doi.org/10.1139/cjfas-2023-0169

11

Table 3. Description of performance metrics with intended objective.

Metric	Description	Equation	Objective	Reference
Cutoff frequency	Number of years age 1+ biomass was below the stock assessment cutoff (150 000 mt) divided by simulation years	$\frac{n_{\text{Age1+}<\text{Cutoff}}}{50}$	Minimize	
Number of cutoff events	Number of events that age 1+ biomass was below the cutoff. An event is the first year of a continuous set of years that biomass was below the cutoff		Minimize	
Closure frequency	Proportion of years TAC = 0		Minimize	
Rebuilding period length	Number of years with age 1+ biomass below the cutoff divided by the number of cutoff events	$\frac{n_{\text{Age1+}<\text{Cutoff}}}{n_{\text{Cutoff}}}$	Minimize	Siple et al. (2019)
Collapse frequency	Years age 1+ biomass was below the collapse threshold (50 000 mt) divided by simulation years	$\frac{n_{\text{Age1+}<\text{Collapse}}}{50}$	Minimize	
Collapse length	Number of years with age 1+ biomass below 50 000 mt divided by the number of collapse events	$\frac{n_{\text{Age1+}<\text{Collapse}}}{n_{\text{Collapse}}}$	Minimize	
Collapse severity	Relative depletion below the collapse threshold, given the stock is collapsed	$1 - (B_{\text{collapse}}/50\,000)$	Minimize	Siple et al. (2019)
Median age 1+ biomass	Median annual biomass of age classes 1 and older over all simulation years		Maximize	
Median catch	Median annual catch over all simulation years		Maximize	
Catch variation	Standard deviation of catches		Minimize	
Cutoff (collapse) error rate	Sum of falsely identified cutoffs (collapses) and missed cutoffs (collapses) in the terminal assessment year divided by the number of converged assessments	$\frac{(\text{FalsePos}+\text{FalseNeg})}{N_{\text{grad}<0.01}}$	Minimize	Piet and Rice (2004)
Missed cutoff (collapse) rate	Number of years in which a converged terminal assessment estimated biomass as above the cutoff (collapse) threshold, given that stock biomass was actually below the threshold, divided by number of years biomass was below the cutoff (collapse) threshold	$\frac{n_{\hat{B}>\text{Cutoff}|\text{Cutoff, grad}<0.01}}{n_{\text{Age1+}<\text{Cutoff}}}$	Minimize	Piet and Rice (2004)
Mean conditional relative error	Mean of relative errors for terminal years for which assessed age 1+ biomass was above the cutoff (closure) threshold given that stock biomass was actually below the threshold		Minimize	

Note: TAC, total allowable catch.

beginning with an early phase of consistently high biomass, followed by a phase of unreasonably high biomass beginning around 2045. Average biomass in both these scenarios reached levels ($>2 \times 10^6$ mt) beyond those estimated in the recent historical period (1981–2019; Kuriyama pers. comm.), as well as biomass estimates during the peak of the fishery in the 1930s and 1940s (Clark and Marr 1955). We therefore treat these as robustness scenarios (sensu Punt et al. 2016a) and will not address their results here but include their output in Figs. S3–S6. Thus, we identify the autocorrelated, MICE, Future PDO, and cyclic PDO scenarios as our reference set of scenarios for the remainder of this study.

Individual biomass trajectories showed realistic boom–bust dynamics within an iteration (colored lines in Figs. 2A and 3). Biomass declines were generally associated with periods of below-average recruitment (i.e., negative recruitment deviations). Figure 3 depicts example trajectories of biomass under the nine HCRs for an iteration in the MICE recruitment scenario. Each trajectory was the product of a common

time series of recruitment deviations, an HCR strategy, and random sampling error. In this example, biomass rebuilt beyond the cutoff threshold (topmost red line), peaked in 2039, and declined below the closure threshold by the late 2050s, even when no fishing occurred (NoCat in Fig. 3). Poor recruitment (deviations <-1.25, indicated with black points in Fig. 3) tended to precede biomass declines, and consecutive years of poor recruitment drove biomass crashes or inhibited recovery of the stock after a decline. Fishing strategies reduced biomass below unfished levels (Fig. 3), with some HCRs driving biomass below cutoff or collapse thresholds (e.g., the index-based (Index) and dynamic 40-10 (Dyn40-10) rules, respectively).

EM fit

Each EM estimated a full trajectory of annual biomasses from 2020 through a terminal year for the simulated stock assessment (2069). Of the assessments with converging

Fig. 6. Relative assessment error in each terminal (assessment) year of the Stock Synthesis estimation model for each reference recruitment scenario under PFMCFSST. Individual boxplots represent error between the assessment estimate of age 1+ biomass for that year and the operating model biomass across iterations. In each plot, the center horizontal bar is the median, hinges represent the 25% and 75% quartiles, and whiskers are the upper and lower 95% confidence intervals.
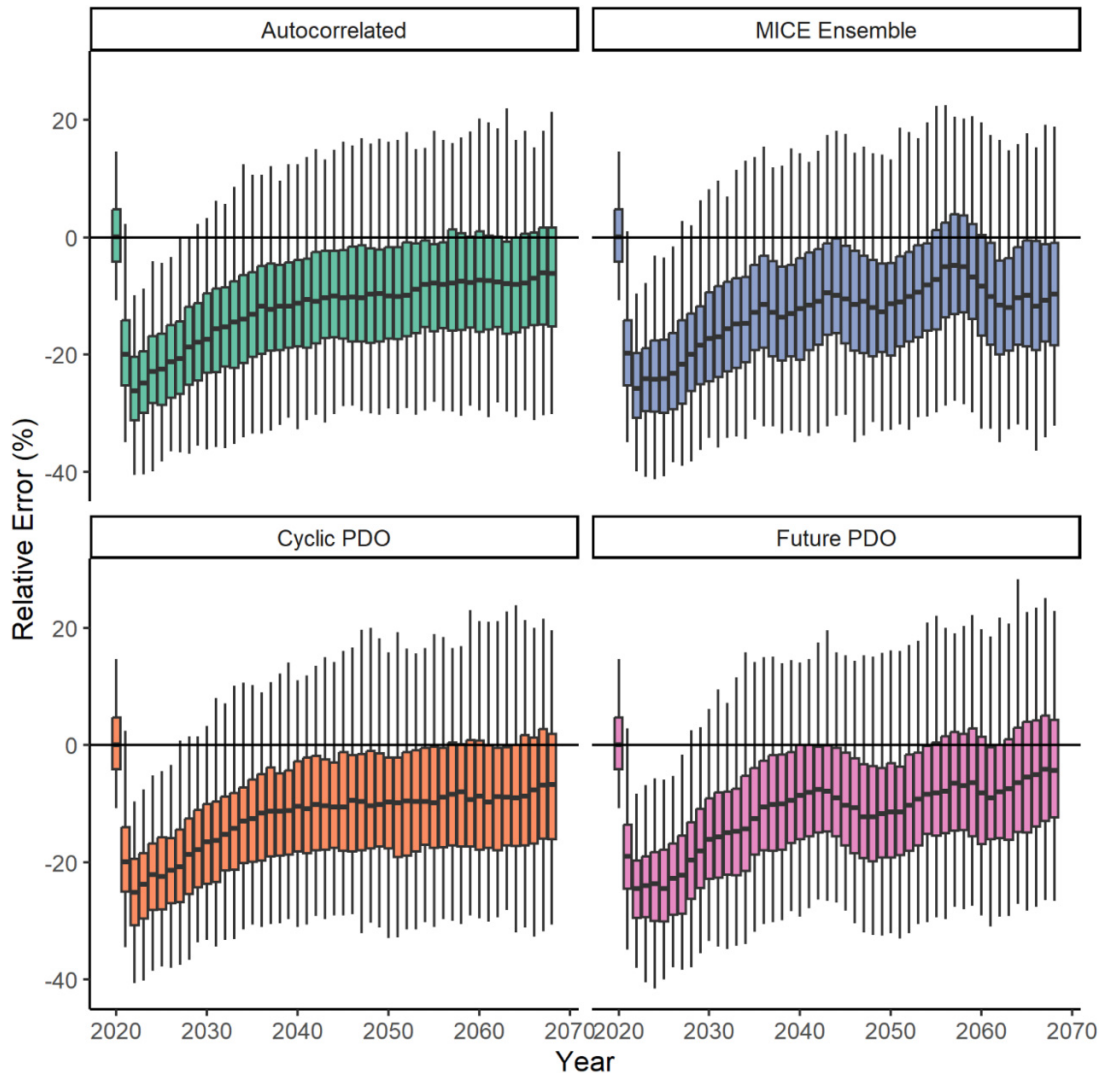
EMs, relative error in the terminal assessment year (i.e., biomass estimated for the year in which the assessment was simulated) was consistently negatively biased (Fig. 6). The negative bias in relative error was reduced toward zero (median $> -20\%$) after the first 15 years of the projection. The negative bias in the terminal assessment year was less extreme when age 1+ biomass was below the 150 000 mt management limit or when recruitment was below 1 SD of the historical recruitment distribution (Fig. 7). In contrast, the CCES index-based biomass estimates, which used simulated acoustic-trawl survey data from the preceding year with error, tended to be positively biased and had higher variation than estimates derived from the EM assessment model (Fig. 7). Though the relative error in an individual recruitment scenario/HCR combination varied, these trends in assessment bias were consistent across scenarios and HCRs. See Figs. S7–S13 for further model diagnostics.

Harvest control rule performance

Fishery and stock status

Our interest here was to compare performance of the HCRs under the climate change (Future PDO and MICE) and no climate change (autocorrelated and cyclic PDO) recruitment scenarios (Table 1) to assess whether management was robust to all potential hypotheses of future climate-driven shifts in recruitment. Therefore, we report aggregate metrics for each HCR with results pooled among our two reference recruitment scenario sets, and we present scenario-specific metrics in Tables S2–S4 and Figs. S14–S26. Compared to variation in performance among scenarios, the median trends in performance were similar among HCRs overall. In the results below, we report patterns in median performance among HCRs for each metric. Complete statistics of performance metric distributions are reported in Table S5. Where contrasts exist,

Fig. 7. Relative assessment error in the terminal (assessment) year of the Stock Synthesis estimation model over reference recruitment scenarios and iterations for assessment years with high (recruitment deviation >1.25, green), average (−1.25 < deviation < 1.25, white), or poor (deviation <−1.25, yellow) recruitment. Terminal year relative error in assessment years with operating model (OM) biomass above the cutoff threshold (age1+ biomass >150 000 mt) is in the top row, and relative errors for assessment years with OM biomass below the cutoff threshold are in the bottom row. Note that for the Index HCR, there is no assessment and errors are calculated from the most recent CCES index value.
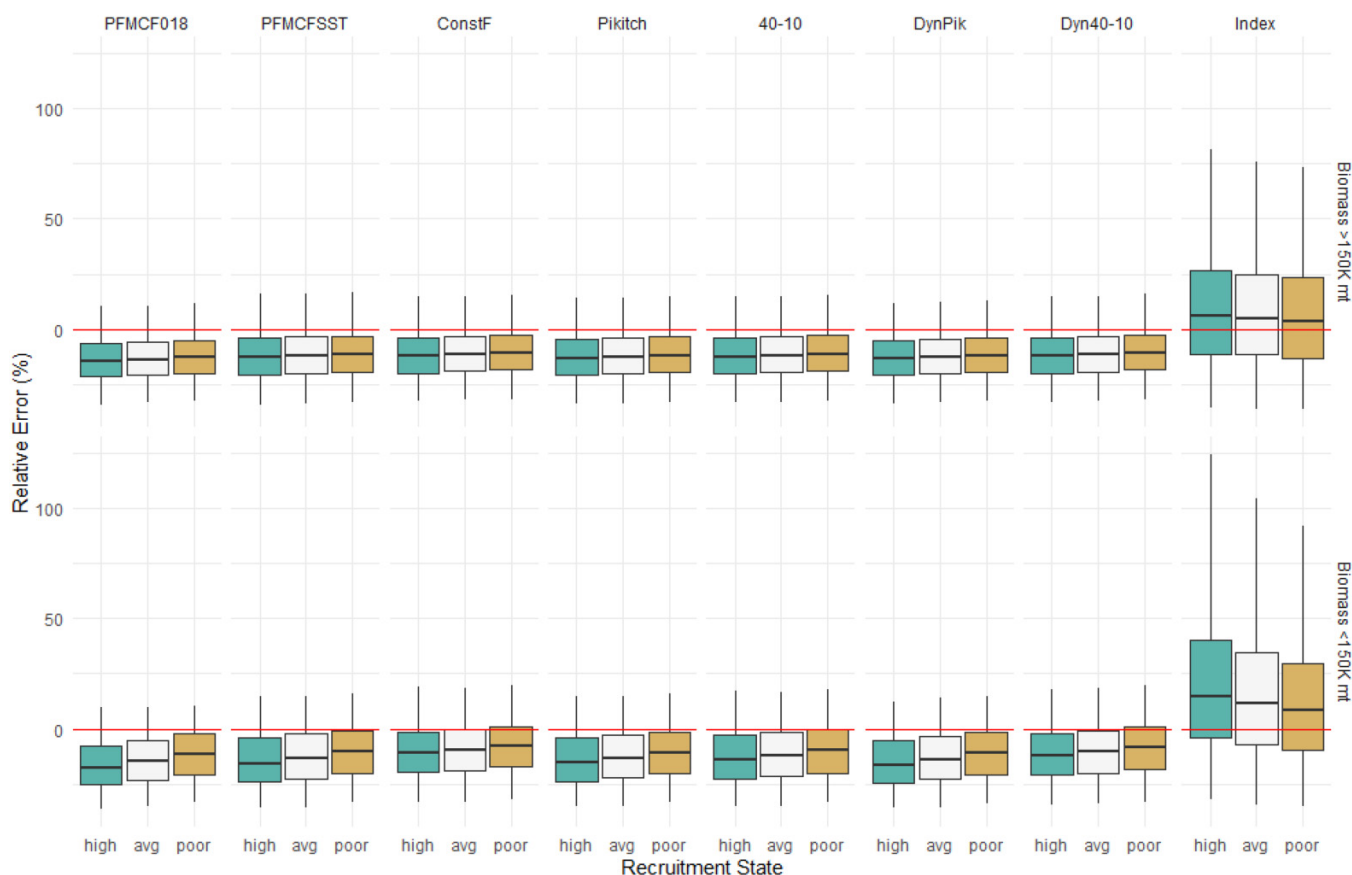
we highlight performance at the 5th or 95th percentile for maximized or minimized metrics, respectively, to emphasize the risk of unfavored outcomes when recruitment drivers are unknown.

In the absence of fishing (NoCat), many performance metrics had more favorable outcomes under the climate change scenarios than in the no climate scenario group (Figs. 8 and 9). This included higher median relative age 1+ biomass (climate: 1.06, no climate: 0.972; Table S5), lower median frequency of being below the cutoff threshold (climate: 0.100; no climate: 0.160), and shorter average rebuilding times (climate: 4 years; no climate: 5 years). Note that even under favorable climate conditions and no fishing, the simulated stock has a low but nonzero chance of declining below the cutoff and collapse thresholds (e.g., median frequency of age 1+ biomass <50 000 mt was 0.060 under a no catch HCR).

There was a clear tradeoff between the median biomass and median catch performance metrics (Figs. 8 and S15). The PFMCF018 rule had the highest fishery closure biomass limit (biomass below which $E = 0$), and was thus the most conservative. Indeed, PFMCF018 performed best among HCRs for biomass conservation under both climate scenarios; the me-

dian age 1+ biomass relative to the mean for the scenario was 0.825 and 0.781 for climate and no climate scenario groups, respectively. Yet, this strategy resulted in the lowest median catch relative to the scenario mean for both scenario groups (climate: 0.682; no climate: 0.532). In contrast, the current SST-based HCR (PFMCFSST) had the lowest median relative age 1+ biomass (climate: 0.672; no climate: 0.645) and the highest median relative catch (climate: 1.11; no climate: 0.827). Similarly, the HCR with constant harvest below the MAXCAT limit (ConstF) had low age 1+ biomass performance (median with and without climate signals: 0.719 and 0.635, respectively), with the highest risk of low biomass levels in both climate scenario groups (5th percentiles: 0.0400 and 0.0348 for climate and no climate, respectively), but high relative catch (median with and without climate signals: 0.977 and 0.899, respectively). Likewise, both Pikitch and DynPik rules, which had a higher threshold and fishery closure biomass than the 40-10 HCRs, performed better than the 40-10 HCRs in terms of biomass but not catch. Unlike for other HCRs, the biomass–catch tradeoff was less clear-cut for the index-based HCR (Index), which applied the PFMCF018 to CCES index data rather than EM output. This HCR had lower

Fig. 8. Annual age 1+ biomass (left) and catch (right) relative to the mean within each reference recruitment scenario: no climate scenario set (autocorrelated and cyclic PDO) in darker colors and climate scenario set (MICE and Future PDO) in lighter colors. The horizontal bar indicates the median value and whiskers are the central 95th percentiles among samples for each metric.
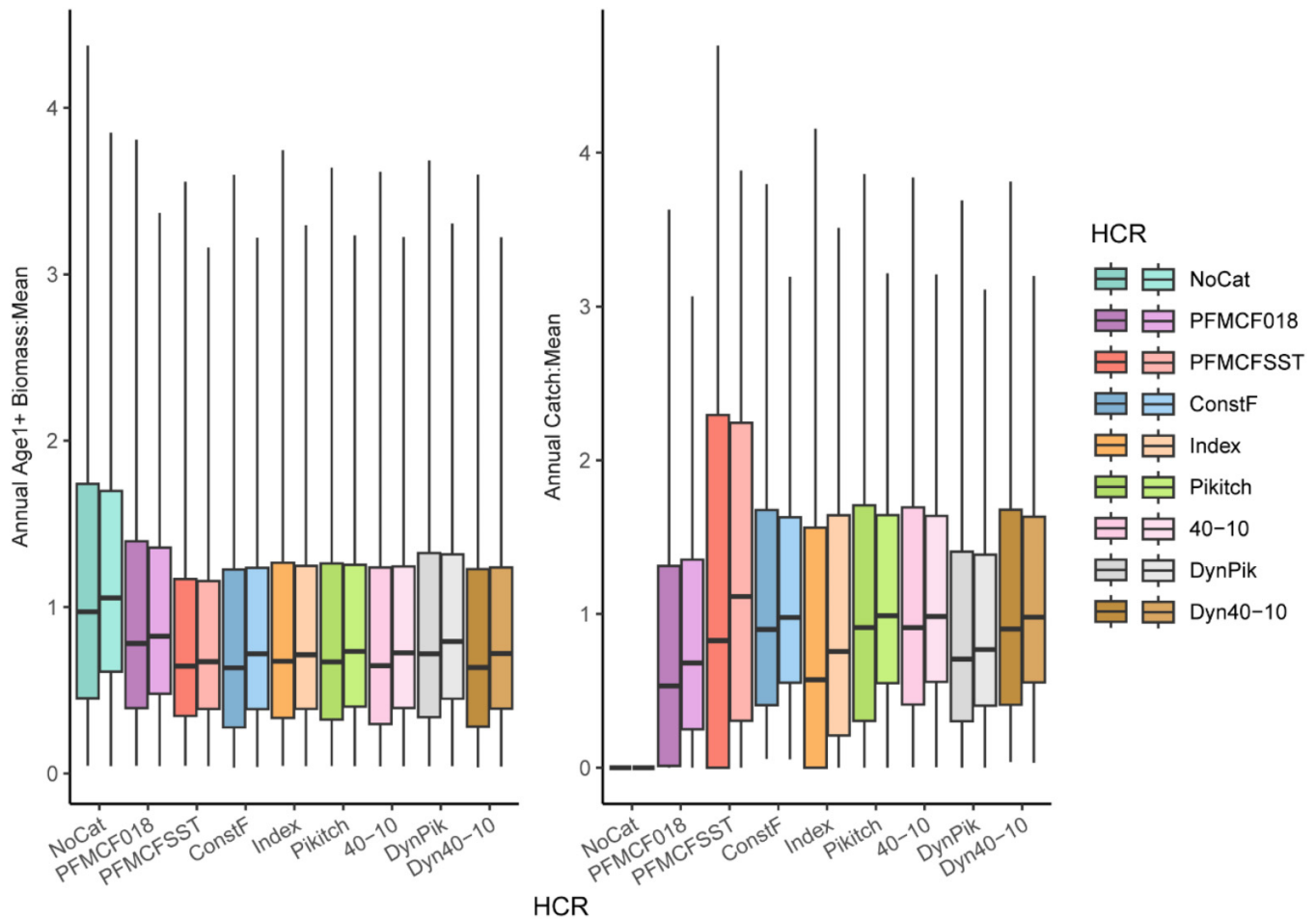

median relative age 1+ biomass (climate: 0.713; no climate: 0.675) but also low median relative catches (climate: 0.757; no climate: 0.573).

The PFMCF018 rule also performed well for the other fishery-related performance metrics (Fig. 9). It was among the best performing HCRs in terms of the median cutoff frequency, number of cutoff events, and mean collapse length under both climate change and non-climate change scenarios. The PFMCF018 HCR also had the lowest risk of age 1+ biomass falling below the cutoff threshold (95th percentile of cutoff frequency with and without climate change: 0.220 and 0.540, respectively). However, this came at the cost of a higher frequency of fishery closures than the constant exploitation (ConstF) or broken stick HCRs. The PFMCFSST HCR was the only rule that had a varying target exploitation rate, which contributed to high values of catch variation under this rule (median climate catch SD: 68 722 mt; no climate: 67 930 mt). This HCR performed generally well for the other performance metrics (Fig. 9) and had short rebuilding lengths (climate: 3.5 years; no climate: 4.5 years) and highest median catches of all HCRs in climate change scenarios (1.11), despite having the highest frequency of fishery closure (Fig. 9G). The

Index HCR had the second highest catch variation (median catch SD with and without climate change: 61 325 and 57 819 mt, respectively) and had the highest median frequency of fishery closures together with the PFMCFSST rule (climate: 0.14; no climate: 0.24 for each HCR).

Both the equilibrium and dynamic B_0 applications of the Pikitch rule performed moderately well (Figs. 8 and 9). The original Pikitch rule (Pikitch) performed similarly to the index rule in both climate change and no climate change contexts, except for the relative catch metric, which was higher than many other HCRs (median relative catch with and without climate change: 0.988 and 0.912, respectively). The dynamic B_0 Pikitch rule (DynPik) had the second highest median relative biomass (climate: 0.794, no climate: 0.719; Fig. 8). These two HCRs also had lower closure frequencies and lower catch SD compared to the PFMC rules and performed better than the 40-10 rules in metrics related to stock biomass. The DynPik rule had fewer closures, number of cutoffs, and instances when biomass <150 000 mt than the equilibrium Pikitch rule but had longer rebuilding length (Fig. 9).

With no cutoff, the constant exploitation HCR (ConstF) performed well in terms of catch (Fig. 8) but was among the

Fig. 9. Boxplots of fishery cutoff (A and F), collapse (B, C, and D), closure (G), rebuilding (E), and catch variability (H) performance metrics are aggregated across years and iterations of the reference recruitment scenarios: no climate scenario set (autocorrelated and cyclic PDO) in darker colors and climate scenario set (MICE and Future PDO) in lighter colors. The horizontal bar indicates the median values and whiskers are central 95th percentiles among samples for each metric.
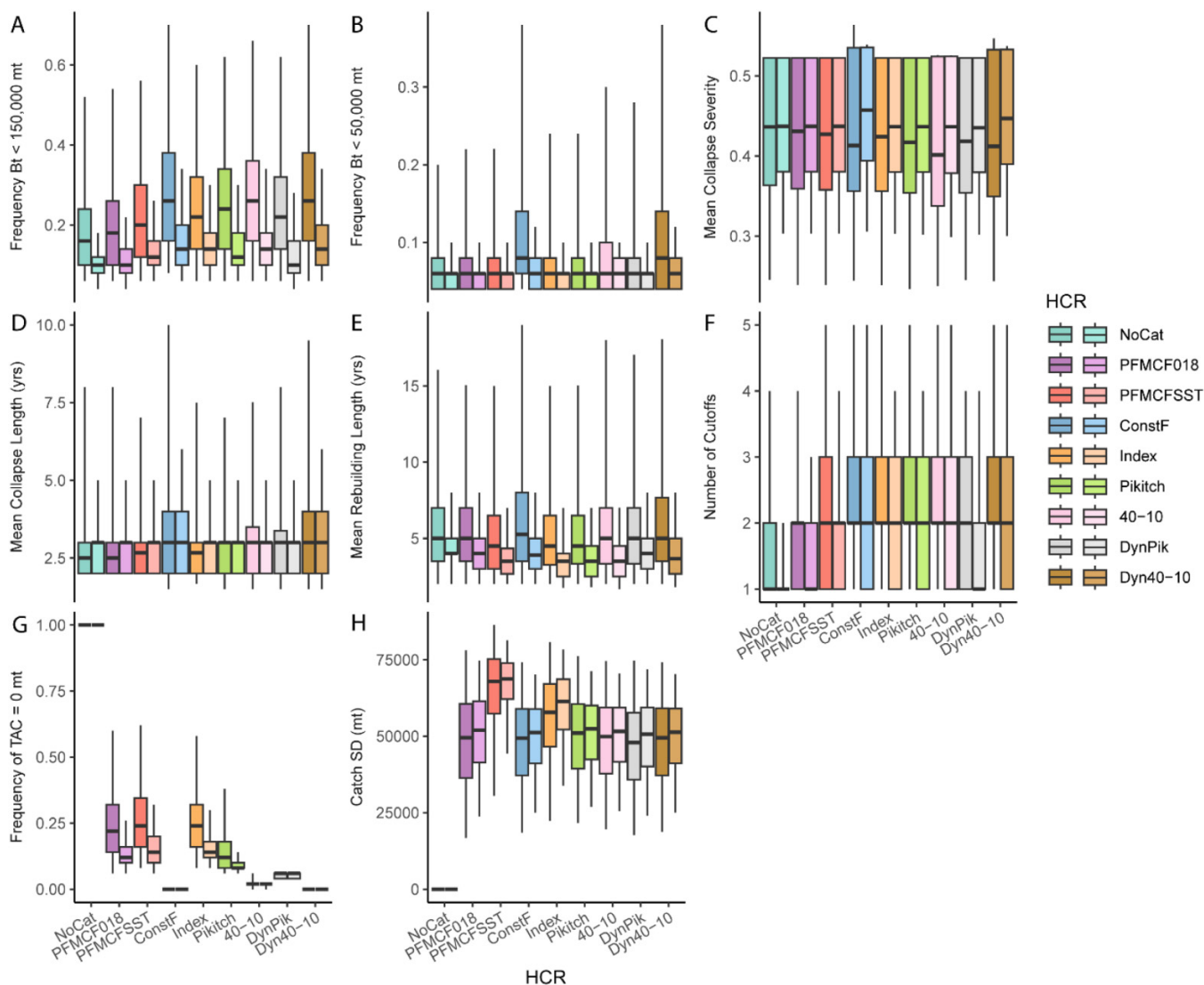
worst performing HCRs for the remaining performance metrics, particularly under a no climate change assumption (e.g., median cutoff frequency: 0.26; median collapse frequency: 0.08; median average rebuilding length: 5.25 years). The equilibrium and dynamic B_0 40-10 HCRs (40-10 and Dyn40-10) also generally performed poorly, grouping with the ConstF rule (Figs. 8 and 9). These rules resulted in high catches and low catch variation, largely because they allowed low levels of catch at small stock sizes rather than closing the fishery. The equilibrium 40-10 rule rarely closed the fishery (closure frequency of 0.02), whereas the dynamic 40-10 rule (Dyn40-10) never closed the fishery completely (Fig. 9G). The 40-10 HCRs had higher risk of collapses, cutoff events, instances of biomass below 150 000 mt, longer and more severe collapses, and longer rebuilding times (95th percentiles in no climate change scenarios: ≥4, ≥0.6, ≥0.26, ≥0.525, ≥6, and ≥14 years, respectively) than other HCRs except for the constant exploitation rule. The dynamic 40-10 rule (Dyn40-

10) performed as poorly as the ConstF rule for cutoff (climate: 0.34; no climate: 0.70) and collapse frequencies (climate: 0.38; no climate: 0.12). This rule also had poor performance for collapse severity (climate: 0.537; no climate: 0.547) and rebuilding length metrics (climate: 8 years; no climate: 18 years).

Cutoff and collapse detection

Overall, our simulated management advice—regarding whether stock size was above or below cutoff and collapse levels—had relatively low error rates. The total error rate for identifying biomass below the cutoff threshold ranged from 1.4% to 6.4%. Total error rate for identifying biomass below the collapse threshold ranged from 0.7% to 2.7% (Figs. 10A and 10D). These error rates were higher under an autocorrelated recruitment scenario and lowest in the scenario with recruitment determined by the MICE ecosystem model.

Fig. 10. Terminal error rates with respect to the cutoff (top row) or collapse (bottom row) thresholds for each HCR and recruitment scenario. The first column (A and D) depicts total errors (Type I and Type II errors), the middle column (B and E) shows error rates for misidentified (missed) cutoffs or collapses, and the right column (C and F) shows the mean relative error of biomass estimates (percentage) conditioned on years when an assessment (or CCES index biomass) misidentified a cutoff or collapse. Note each panel uses a different *y*-axis scale.
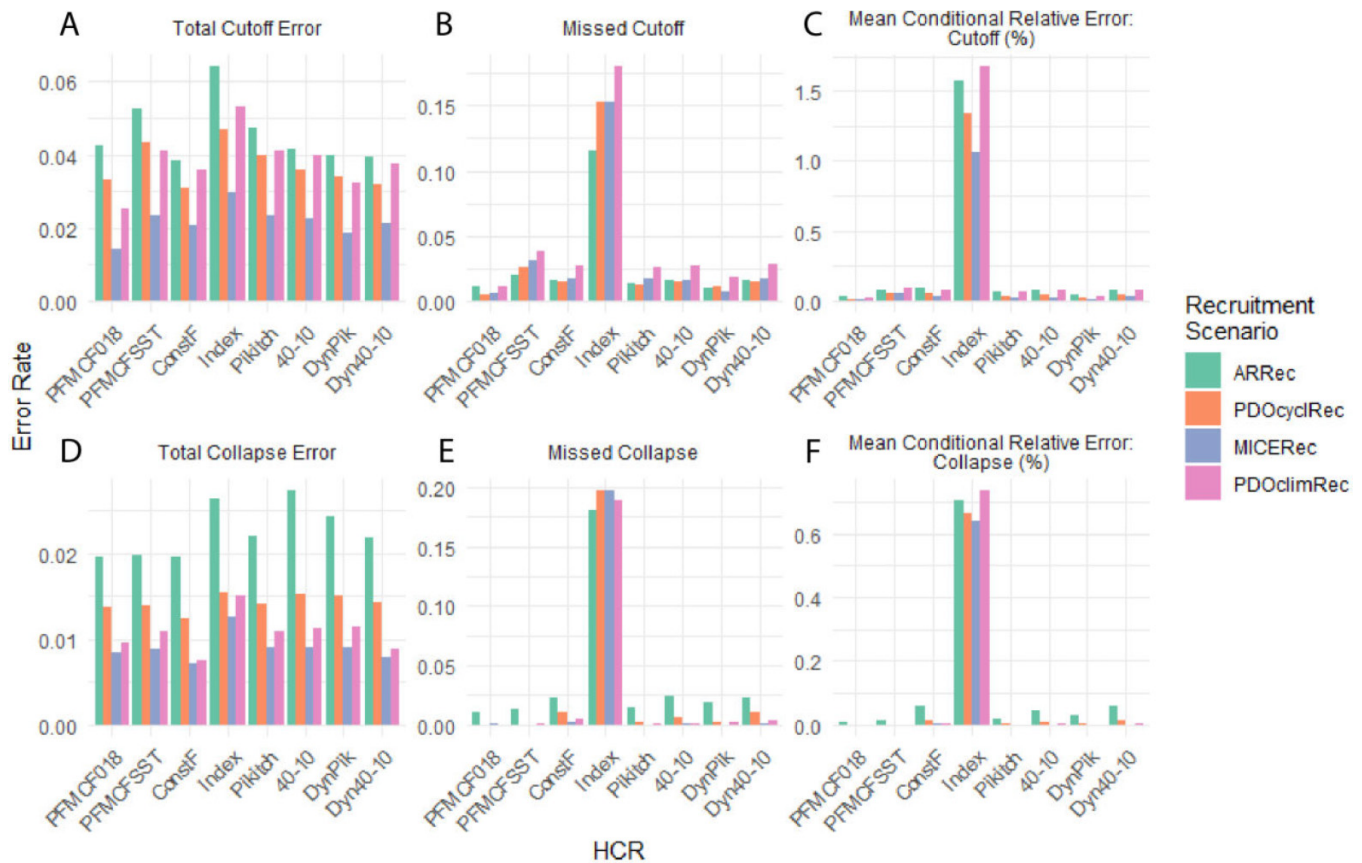
Perhaps, the most critical management advice relates to the (EM) assessment of stock status in years for which the "true" (OM) age 1+ biomass was below the cutoff threshold. In these years, the average false negative error rate, or rate of misidentifying that stock was below the cutoff, ranged from 0.5% to 3.8% for the HCRs using biomass estimates from the EM model (Fig. 10B). The relative magnitude of these errors, conditioned on biomasses below the threshold, was quite small (<0.1% mean relative error, Fig. 10C). In contrast, the Index HCR that used the CCES index data for decision-making had higher mean error rates (11.5%–18.0%), an order of magnitude larger than the assessment-based HCRs, with mean relative error in the magnitude of estimated biomass between 1% and 2% (Fig. 10C). This is consistent with the higher terminal year error when applying the Index HCR (Fig. 7). These same patterns existed for errors measured around the collapse threshold, though some HCRs (PFMCF018, PFMCFSST, Pikitch, and DynPik) never missed a biomass collapse under the MICE, cyclic PDO, and (or) Future PDO recruitment scenarios (i.e., false negative rates were 0; Fig. 10E). These false negative error rates occurred between 18.0% and 19.6% of the projection years for the index-based HCR, though the magnitude of these biomass estimate errors were smaller than in the case of the cutoff threshold (0.64%–0.73%; Fig. 10F). The

full contingency tables for cutoff and collapse thresholds are included in Tables S6 and S7.

Discussion

Through MSE, we tested the robustness of the PFMC's SST-based sardine HCR, along with alternatives, to recruitment variability, including climate-driven scenarios. Results were largely consistent across climate change and non-climate change scenarios. For instance, the HCR that performed best under the climate change scenarios in terms of the biomass also performed best for biomass in the no climate change runs. All HCRs performed better under the climate change scenarios as the climate-driven recruitment projections implied a more productive stock. No HCR performed best across all performance indicators as tradeoffs were evident between catch and biomass metrics. Threshold harvest control rules fishing at E_{MSY} (PFMCF018) or linked to SST (PFMCFSST) and a dynamic B_0 implementation of Pikitch et al.'s (2012) rule (DynPik) performed the best based on maximizing stock biomass, catch, or reducing catch variation, respectively. Taken together, these HCRs had the following characteristics: (1) a higher stock biomass limit under which fishery closures preserved reproductive potential at low biomass, (2)

use of a statistical stock assessment model to reduce estimation error, and (3) dynamic response either to latent states estimated by a stock assessment model or to environmental variables external to the assessment. Because performance varied more among recruitment scenarios (climate versus no climate recruitment scenario sets) than among HCRs, our MSE also suggests that, along with regular monitoring and assessment, management success may depend more on understanding and modeling drivers of climate-driven changes in recruitment dynamics than on refining HCR functional form.

The review by Deroba and Bence (2008), summarized in Fig. 4, helps to interpret differences in performance between the HCRs tested here and to compare our results to those from the MSE of Hurtado-Ferro and Punt (2014), on which the current SST-based HCR was based. In their study, Hurtado-Ferro and Punt (2014) contrast performance of HCRs that (1) use either constant or variable E_{target} rates, and if variable, what range these rates were allowed to vary over, (2) the influence of a maximum catch cap, and (3) the level of B_{limit} (i.e., CUTOFF), which was implemented as a threshold HCR and set equal to $B_{trigger}$. The HCR implemented in the PFMC fishery management plan for Pacific sardine (PFMCFSST in this study) is a threshold HCR with $B_{limit} = B_{trigger} = 150\,000$ mt, and has a maximum catch cap and a variable E_{target} based on SST. Our study highlights the value of a well-selected B_{limit} and the influences of dynamic reference points (e.g., environmentally informed E_{target} or dynamic B_0), which are features of the HCRs implemented in the present study.

The current SST-based HCR (PFMCFSST) consistently delivered higher catches over the 50-year simulation with the tradeoff of having lower stock biomass, higher catch variation, and more frequent closures compared to an HCR with a stationary E_{target} of E_{MSY}. Higher catch variation under the SST-based HCR was likely due to the combination of varying target harvest levels that allow higher catch rates at warm temperatures and to smaller stock sizes on average leading to more frequent fishery closures compared to the stationary E_{MSY} rule. As in our analysis, Hurtado-Ferro and Punt's (2014) original MSE for this stock found that there was no best performing HCR due to tradeoffs between management objectives. The temperature-informed HCR (their variant 6) and a stationary E_{target} HCR (their variant 18) performed decently for both mean catch and mean age 1+ biomass performance metrics. The tradeoffs between these metrics for these HCRs were reversed in their analysis, but the differences were not as great as we saw in this study. Further, the rank order of these and a constant exploitation HCR (their variant 4) was similar to the corresponding HCRs in this study (ConstF) for metrics on variation in catch and frequency of falling below the 150 000 mt cutoff threshold (Hurtado-Ferro and Punt 2014). It should be noted that unlike in this study, their SST E_{target} was capped at 0.15 and a broader range of implementation and biological uncertainties was tested. This suggests that the MSE approach used here to compare HCR performance can identify rules that lie at extremes of tradeoff frontiers, but that finer differentiation of performance between similar HCRs is likely influenced by uncertainties resulting from model structure decisions made when defining OM and HCR implementation scenarios in the analyses.

Therefore, any management decisions about the HCRs evaluated here should be based on further modeling accounting for model structural sensitivities as was done before selecting the current PFMC HCR (Hurtado-Ferro and Punt 2014).

In contrast to the PFMC sardine HCRs, the Pikitch et al. (2012) rule resulted in moderate performance across all metrics investigated in our analysis. This may be due to the shape of this rule compared to the PFMC rules. In the equilibrium Pikitch case, the closure threshold ($B_{limit} = B_0 * 0.4 \approx 125\,500$ mt) was slightly lower than the 150 000 mt closure limit of the PFMC rules and the trigger biomass ($B_{trigger} = B_0 * 0.8 \approx 251\,000$ mt) began reducing fishing pressure at much higher biomass levels. This gradual reduction of exploitation rate at higher biomasses helped conserve more spawning biomass, particularly when recruitment was poor, thus reducing variation in catch by avoiding large changes in biomass and consequently avoiding fishery closure more often than the cliff's-edge style PFMC rules. In particular, the dynamic Pikitch rule (DynPik) exhibited relatively high biomass and catch, with low catch variation and collapse and closure frequencies across all our reference recruitment scenarios. When using a dynamic B_0 reference point, the level of exploitation is based on current reproductive capacity of the stock. Thus, the dynamic B_0 HCR reduced the frequency of both closures and cutoffs as compared to the equilibrium B_0 rule. This supports other studies suggesting that using reference points with respect to a dynamic B_0 may improve fishery performance under time-varying productivity relative to static reference points for some species (Berger 2019; O'Leary et al. 2020; Bessell-Browne et al. 2022). Although the dynamic Pikitch rule does not perform best for most metrics, it may reduce the distinct fishery versus conservation tradeoffs demonstrated in the PFMC HCRs, leading to sufficient outcomes overall. Our results also mirror Berger's (2019) findings that recruitment dynamics may swamp distinctions between dynamic or equilibrium B_0 performance, as differences in performance metrics among the dynamic and equilibrium Pikitch HCRs investigated here shrank in our climate-influenced recruitment scenarios compared to our no climate change scenarios.

The remaining HCRs generally grouped together and had poor performance for more than one performance metric. Fishing at a constant harvest rate below the maximum catch limit (ConstF) resulted in the highest risk of crossing cutoff and collapse thresholds and led to delayed rebuilding of the stock. Siple et al. (2019) also highlight that, for forage fish, low constant exploitation rules, while enhancing stability and catch metrics, increased risk of collapse. The 40-10 rule had similarly poor performance because of a low closure threshold ($B_{limit} = B_0 * 0.1 \approx 31\,400$ mt) and of $B_{trigger}$ below the biomass that the current PFMC HCR closes the fishery ($B_{trigger} = B_0 * 0.4 \approx 125\,500 < 150\,000$ mt). Because of the low reference points applied in this study, neither the equilibrium or dynamic 40-10 rules implemented fishery closures regularly and thus acted similarly to the constant exploitation HCR. Also, distinctions in performance of the dynamic versus equilibrium 40-10 rule implementations cannot be easily determined as the reference points were rarely triggered. Although Siple et al. (2019) do not apply

the 40-10 rule as done here, they test a rule with the same $B_{limit} = 0.1B_0$ and a higher $B_{trigger} = 0.8B_0$ (corresponding to our Pikitch rule $B_{trigger}$) and found it improved performance over the standard Pikitch rule for some metrics. Thus, early reduction of harvest rates in a broken-stick rule with a high $B_{trigger}$ may allow use of a lower B_{limit} than threshold rules, but further MSE explicitly testing the effects of placement of B_{limit} with the same $B_{trigger}$ is needed to explore this further.

Unique among the HCRs, the index-based application of the stationary E_{MSY} HCR (Index) had much higher relative error rates, leading to a failure to detect 10% of the cases when the stock was below the cutoff threshold. Considering the successful use of index-based HCRs in other small pelagics fisheries (e.g., South Africa and Peru), we provide a discussion of caveats related to our application of this approach in the present study. We note that the root of poor performance for this strategy stems from observation error applied to the CCES biomass index, which is not reduced through an assessment. Catch guidance for our Index HCR is based on survey data sampled a year before the beginning of the new TAC year, reflecting current sampling limitations for this stock (Fig. 1). By contrast, fisheries that have implemented an index-based decision rule base their catch levels off pre-season surveys that reflect more recent stock status than the CCES index simulated here (e.g., South Africa's sardine and anchovy; de Moor 2018). Application of this type of strategy in the California Current would be challenging given the timelines for when surveys are conducted and when catch limits are set according to the PFMC process. Further, we implemented a consistent 25% CV log-normal error around our CCES index throughout our simulation, compared to summer survey CVs greater than 30% used in the PFMC stock assessment (Kuriyama et al. 2020). Future investigations into an index-based approach might increase CV values as biomass decreases. When sardine abundance is low, distribution becomes patchy, resulting in higher CVs. For example, in the recent northern Pacific sardine stock assessment, one CCES index observation had a biomass estimate of 751 075 mt with a CV of 0.09 and another value had a biomass of 16 375 with a CV of 0.94 (Kuriyama et al. 2020). Thus, future MSE analyses investigating the influence on survey index timing and effects of density-dependent sampling error may provide a more realistic characterization of the sampling process and risks to providing advice for management.

This final insight reveals how the error structure of an assessment can affect its performance in providing management advice. Because of limited computing resources, previous MSEs in this and other systems have often sampled population biomass with error, resulting in a biomass index (similar to a fishery-independent survey) rather than passing sampled data to an EM (e.g., Hurtado-Ferro and Punt 2014; Punt et al. 2016b; Siple et al. 2019). With our approach using the SSMSE package and fitting a Stock Synthesis model to the simulated data, we revealed that the simplifying approach of accounting for assessment error by adding a random error to the biomass output from the OM may miss important error patterns and bias in the assessment that impact management advice and thus the effectiveness of the HCR applied. With the full assessment approach afforded by

SSMSE, we showed that the biomass estimates in the final year of the assessment were negatively biased. We note that the negative bias pattern in age 1+ biomass estimates for the terminal year for our study (Fig. 6), and from a survey index (positive, Fig. 6) is case-specific and more simulation studies are needed to understand the sources and broader implications of biomass estimation bias. We suspect that negatively biased terminal year biomass estimates are tied to the highly uncertain recruitment estimates for the last years of the EM, which in turn are dependent on the timing of available observations relative to the terminal year, availability of young-of-the-year sardine to the survey and fisheries, the assumed constant CCES index CV discussed above, and the observation error assumed for age and length compositions. For instance, due to the lack of information on recent recruitment in the data, terminal year EM recruitment estimates are highly uncertain with a mean close to the average from the stock recruitment relationship. This leads to large bias in terminal recruitment estimates from the EM as compared to the OM, which is particularly evident and negative during years of high recruitment (Fig. S8). We suspect that this bias in the most recent recruitment estimates from the EM is associated with the negative bias in age 1+ biomass. Support for this argument may be found in the lack of bias in the age 1+ biomass estimate for the first projection year (2020, Fig. 6), which relies on the final year of observations included in the conditioning period and is not yet affected by errors in the estimation of the 2020–2069 simulated recruitment deviations. However, for a full evaluation of causes of bias and its relationship to EM model formulation and data availability, we would need to conduct further simulations with different data input combinations that were out of the scope of the current work. This estimation bias had consequences for the HCRs that then used these estimates to advise management, which were different from those taken from advice that is generally unbiased overall but less certain (i.e., wider confidence intervals). This negative biomass bias in the final assessment year also led to more precautionary catch advice in simulations using this output, leading to threshold detection error rates that were imbalanced between false positives and false negatives for these HCRs. Our methods allowed us not only to measure the effectiveness of the management strategies applied in our MSE, but also the effectiveness of the assessment model itself. We encourage the use of these and other innovative tools to explore these questions further.

The EM in this study represented a simplification of the stock assessment used for management (and likely the variability in multiple biological processes). These simplifications were used because the focus here was to evaluate the performance of HCRs under different future recruitment scenarios. There is likely time-varying growth and movement for sardine (McDaniel et al. 2016; Kamimura et al. 2022). The management assessment accounts for this with empirical weight-at-age input and by estimating time-varying age-based selectivity. The relationship of warming temperatures and other future environmental conditions between growth and movements is unknown, and as a result was not the focus of the analysis here.

This simulation approach could be expanded to allow direct evaluation of the benefit to management of recruitment indicators for improving assessment biomass estimates and short-term forecasting of fisheries activities. The poorer performance of our lagged Index HCR is not surprising given the highly variable dynamics of this stock. Accurate estimates of the fishable biomass are a persistent need for effective management of forage fish. As described above, in many systems, this has been addressed by developing an adaptive management framework where catch guidance is revised multiple times per year based on frequent, direct estimates of biomass from hydroacoustic surveys (de Moor and Butterworth 2016; Uriarte et al. 2023). In lieu of observations, indicators of recruitment can also provide a timelier estimate of incoming age 0 biomass and input as an additional survey index in the assessment to improve quality of biomass estimates (e.g., Crone et al. 2019). Performance of an assessment that uses environmental or other survey data as a recruitment index could be evaluated using the methods we apply here. Alternatively, as for the Pacific sardine PFMC HCR or Irish Sea herring (Bentley et al. 2021), reference points in the HCR itself (e.g., E_{target}) can be linked to an indicator to ensure catch limits track the productivity of the stock. Furthermore, as a TAC is often based on an estimate of forecast (rather than current) biomass, for these fast-growing species, management outcomes can be improved when the indicator is accurately forecast in advance and both the reference point and biomass forecast reflect near-term recruitment conditions (Tommasi et al. 2017).

Success of indicator-based rules is predicated on a good understanding of and strong relationship between recruitment and environmental drivers (Haltuch et al. 2019*b*). A direct SST–recruitment relationship was not included in our reference set of scenarios as the Future SST scenario resulted in unreasonably high biomass levels. The link to recruitment assumed in this scenario was based on the linear effect of temperature on recruitment used to develop the PFMC's SST-based HCR (PFMC 2013; Hurtado-Ferro and Punt 2014). However, the downscaled earth system models project higher future temperatures than have been observed during the calibration period of this relationship. An improved Future SST scenario could thus enforce a limit on the positive linear SST–recruitment relationship as would be implemented in a shape-constrained thermal niche species distribution model approach (Citores et al. 2020; Muhling et al. 2020). Increased stock productivity was also simulated in the regime recruitment scenario, which added a positive scalar to recruitment deviations. Because small pelagic fish stock dynamics are highly sensitive to the formulation of the stock–recruit relationship, this simple modification may not have provided a reasonable depiction of dynamics under a positive recruitment regime and led to unreasonably high biomass levels. We note that we also tested a negative recruitment regime scenario where recruitment deviations were simulated to decrease rather than increase from the initial recruitment regime. However, many HCRs in this negative recruitment regime scenario minimally achieved management objectives (see Tables S4 and S5). We found that

use of recruitment deviations derived from a mechanistic model that explicitly incorporates multiple processes and drivers affecting recruitment, our MICE recruitment scenario (Koenigstein et al. 2022), is a promising approach to generate more realistic scenarios of recruitment under climate change for MSE than those derived from correlative methods.

Temperature did indirectly inform the climate-driven PDO recruitment (PDO is based on North Pacific SST) and MICE model recruitment scenarios (in the MICE, recruitment is dependent on SST as well as food availability; Koenigstein et al. 2022). Because of the positive relationship between temperature (and forage) and recruitment in these scenarios, biomass was projected to increase under climate change, increasing the performance of all HCRs in this set of scenarios. We note that this assumption may not hold in the natural system, which is more complex than that modeled here. For sardine, the SST–recruitment relationship through PDO is changing (Zwolinski and Demer 2019), and high ocean temperatures may impact plankton production, reducing forage for larval and juvenile sardines (Gómez-Ocampo et al. 2018; Brodeur et al. 2019; Koenigstein et al. 2022). In all scenarios, the PFMCF-SST rule performed best in terms of catches, but worse than the corresponding stationary E_{target} rule (PFMCF018) in most other metrics. The ability to increase catches during favorable periods came at the cost of higher catch variability and increased frequency of fishery closures. If (or when) new recruitment indices become available for these highly dynamic stocks, future studies can use the tool developed here to evaluate their value for management decision-making and near-term stock forecasting.

This MSE framework allowed us to investigate the dynamics between forage fish population dynamics and fisheries management. The model dynamics we report here reflect the patterns found in natural fish stocks and support the conclusions of Essington et al. (2015) and Szuwalski and Hilborn (2015) that forage fish stock declines are preceded by years of poor recruitment and can be exacerbated by fishing mortality. With this framework, single species approaches for ecosystem-based fishery management can be developed and tested in the statistically rigorous manner with which fisheries managers are familiar while accounting for the wider ecosystem influences that drive small pelagic fishes.

Acknowledgements

Article information

History dates

Notes

This paper is part of a special issue entitled "Small Pelagic Fishes: New Frontiers in Science for Sustainable Management".

Copyright

Data availability

Code and data generated or analyzed during this study are available in the SardineMSE repository at https://github.com /futureseas/SardineMSE.

Author information

Author ORCIDs

Robert P. Wildermuth https://orcid.org/0000-0002-4539-9321
Desiree Tommasi https://orcid.org/0000-0003-4027-6047
Peter Kuriyama https://orcid.org/0000-0002-6971-4015
Isaac Kaplan https://orcid.org/0000-0002-8748-329X

Author contributions

Conceptualization: RPW, DT, PK, JS, IK
Data curation: RPW, PK
Funding acquisition: DT, IK
Formal analysis: RPW, PK
Investigation: RPW, DT
Methodology: RPW, DT, JS, IK
Project administration: DT
Resources: DT
Software: RPW, DT, PK
Supervision: DT, IK
Validation: PK
Visualization: RPW, PK, JS, IK
Writing – original draft: RPW, DT, PK
Writing – review & editing: RPW, DT, PK, JS, IK

Competing interests

The authors declare there are no competing interests.

Funding information

Supplementary material

Supplementary data are available with the article at https: //doi.org/10.1139/cjfas-2023-0169.

References

Anstead, K.A., Drew, K., Chagaris, D., Schueller, A.M., McNamee, J.E., Buchheister, A., et al. 2021. The path to an ecosystem approach for forage fish management: a case study of Atlantic menhaden. Front. Mar. Sci. **8**: 607657. doi:10.3389/fmars.2021.607657.

Basson, M. 1999. The importance of environmental factors in the design of management procedures. ICES J. Mar. Sci. **56**(6): 933–942. doi:10.1006/jmsc.1999.0541.

Baumgartner, T.R., Soutar, A., and Ferreira-Bartrina, V. 1992. Reconstruction of the history of Pacific sardine and northern anchovy populations over the past two millennia from sediments of the Santa Barbara basin, California. CalCOFI Rep. **33**: 24–40.

Bentley, J.W., Lundy, M.G., Howell, D., Beggs, S.E., Bundy, A., De Castro, F., et al. 2021. Refining fisheries advice with stock-specific ecosystem information. Front. Mar. Sci. **8**: 602072. doi:10.3389/fmars.2021.602072.

Berger, A.M. 2019. Character of temporal variability in stock productivity influences the utility of dynamic reference points. Fish. Res. **217**: 185–197. doi:10.1016/j.fishres.2018.11.028.

Bessell-Browne, P., Punt, A.E., Tuck, G.N., Day, J., Klaer, N., and Penney, A. 2022. The effects of implementing a 'dynamic B0' harvest control rule in Australia's southern and eastern scalefish and shark fishery. Fish. Res. **252**: 106306. doi:10.1016/j.fishres.2022.106306.

Brodeur, R.D., Auth, T.D., and Phillips, A.J. 2019. Major shifts in pelagic micronekton and macrozooplankton community structure in an upwelling ecosystem related to an unprecedented marine heatwave. Front. Mar. Sci. **6**: 212. doi:10.3389/fmars.2019.00212.

Brosset, P., Smith, A.D., Plourde, S., Castonguay, M., Lehoux, C., and Van Beveren, E. 2020. A fine-scale multi-step approach to understand fish recruitment variability. Sci. Rep. **10**: 16064. doi:10.1038/s41598-020-73025-z. PMID: 32999410.

Chavez, F.P., Ryan, J., Lluch-Cota, S.E., and Niquen, C.M. 2003. From anchovies to sardines and back: multidecadal change in the Pacific Ocean. Science, **299**(5604): 217–221. doi:10.1126/science.1075880. PMID: 12522241.

Checkley, D.M., Jr., Asch, R.G., and Rykaczewski, R.R. 2017. Climate, anchovy, and sardine. Annu. Rev. Mar. Sci. **9**: 469–493. doi:10.1146/annurev-marine-122414-033819. PMID: 28045355.

Citores, L., Ibaibarriaga, L., Lee, D.J., Brewer, M.J., Santos, M., and Chust, G. 2020. Modelling species presence–absence in the ecological niche theory framework using shape-constrained generalized additive models. Ecol. Model. **418**: 108926. doi:10.1016/j.ecolmodel.2019.108926.

Clark, F.N., and Marr, J.C. 1955. Population dynamics of the Pacific sardine. CalCOFI Rep. **4**: 11–48.

Cowan, J.H., Jr., and Shaw, R.F. 2002. Recruitment. *In* Fishery science: the unique contribution of early life stages. *Edited by* L.A. Fuiman and R.G. Werner Blackwell Science, Oxford. pp. 88–111.

Crone, P.R., Maunder, M.N., Lee, H., and Piner, K.R. 2019. Good practices for including environmental data to inform spawner–recruit dynamics in integrated stock assessments: small pelagic species case study. Fish. Res. **217**: 122–132. doi:10.1016/j.fishres.2018.12.026.

Cury, P.M., Boyd, I.L., Bonhommeau, S., Anker-Nilssen, T., Crawford, R.J., Furness, R.W., et al. 2011. Global seabird response to forage fish depletion—one-third for the birds. Science, **334**(6063): 1703–1706. doi:10.1126/science.1212928. PMID: 22194577.

de Moor, C. 2018. The 2018 operational management procedure for the South African sardine and anchovy resources. Faculty of Science, Department of Mathematics and Applied Mathematics. Available fom http://hdl.handle.net/11427/33220 [accessed 6 October 2023].

de Moor, C.L., and Butterworth, D.S. 2016. Incorporating technological interactions in a joint management procedure for South African sardine and anchovy. *In* Management science in fisheries: an introduction to simulation-based methods. *Edited by* C.T.T. Edwards and D.J. Dankel Routledge, London. pp. 205–231.

Deroba, J.J., and Bence, J.R. 2008. A review of harvest policies: understanding relative performance of control rules. Fish.Res. **94**(3): 210–223. doi:10.1016/j.fishres.2008.01.003.

Doering, K., and Vaughan, N. 2022. SSMSE: management strategy evaluation (MSE) using Stock Synthesis (SS). R package version 0.2.5. Available from https://github.com/nmfs-fish-tools/SSMSE [accessed 6 October 2023].

Dorval, E., Macewicz, B.J., Griffith, D.A., Lo, N.C.H., and Gu, Y. 2014. Spawning biomass of Pacific sardine (*Sardinops sagax*) estimated from the daily egg production method off California in 2013. U.S. Department of Commerce, NOAA Technical Memorandum NMFS-SWFSC-535.

Essington, T.E., Moriarty, P.E., Froehlich, H.E., Hodgson, E.E., Koehn, L.E., Oken, K.L., et al. 2015. Fishing amplifies forage fish population col-

Can. J. Fish. Aquat. Sci. **00**: 1–23 (2023) | dx.doi.org/10.1139/cjfas-2023-0169

21

lapses. Proc. Natl. Acad. Sci. **112**(21): 6648–6652. doi:10.1073/pnas.1422020112.

Fiechter, J., Rose, K.A., Curchitser, E.N., and Hedstrom, K.S. 2015. The role of environmental controls in determining sardine and anchovy population cycles in the California Current: analysis of an end-to-end model. Prog. Oceanogr. **138**: 381–398. doi:10.1016/j.pocean.2014.11.013.

Food and Agriculture Organization. 2022. The State of World Fisheries and Aquaculture 2022. Towards Blue Transformation. FAO, Rome. doi:10.4060/cc0461en.

Free, C.M., Jensen, O.P., and Hilborn, R. 2021. Evaluating impacts of forage fish abundance on marine predators. Conserv. Biol. **35**(5): 1540–1551. doi:10.1111/cobi.13709.

Gómez-Ocampo, E., Gaxiola-Castro, G., Durazo, R., and Beier, E. 2018. Effects of the 2013–2016 warm anomalies on the California Current phytoplankton. Deep Sea Res. Part II Top. Stud. Oceanogr. **151**: 64–76. doi:10.1016/j.dsr2.2017.01.005.

Haltuch, M.A., A'mar, Z.T., Bond, N.A., and Valero, J.L. 2019a. Assessing the effects of climate change on US West Coast sablefish productivity and on the performance of alternative management strategies. ICES J. Mar. Sci. **76**(6): 1524–1542. doi:10.1093/icesjms/fsz029.

Haltuch, M.A., Brooks, E.N., Brodziak, J., Devine, J.A., Johnson, K.F., Klibansky, N., et al. 2019b. Unraveling the recruitment problem: a review of environmentally-informed forecasting and management strategy evaluation. Fish. Res. **217**: 198–216. doi:10.1016/j.fishres.2018.12.016.

Hewitt, R.P. 1988. Historical review of the oceanographic approach to fishery research. CalCOFI Rep. **29**: 27–41.

Hill, K.T., Crone, P.R., Lo, N.C.H., Macewicz, B.J., Dorval, E., McDaniel, J.D., et al. 2011. Assessment of the Pacific sardine resource in 2011 for U.S. management in 2012. U.S. Department of Commerce, NOAA Technical Memorandum NMFS-SWFSC-487.

Hjort, J. 1914. Fluctuations in the great fisheries of northern Europe viewed in the light of biological research. ICES, **20**: 1–228.

Houde, E.D. 1987. Fish early life dynamics and recruitment variability. Am. Fish. Soc. Symp. **2**: 17–29.

Hurtado-Ferro, F., and Punt, A.E. 2014. Revised analyses related to Pacific sardine harvest parameters. Pacific Fishery Management Council, Portland, OR.

ICES. 2013. Report of the Workshop on Guidelines for Management Strategy Evaluations (WKGMSE), 21–23 January 2013. International Council for the Exploration of the Sea, Copenhagen, Denmark.

Jacobson, L.D., and MacCall, A.D. 1995. Stock–recruitment models for Pacific sardine (*Sardinops sagax*). Can. J. Fish. Aquat. Sci. **52**(3): 566–577. doi:10.1139/f95-057.

Kamimura, Y., Tadokoro, K., Furuichi, S., and Yukami, R. 2022. Stronger density-dependent growth of Japanese sardine with lower food availability: comparison of growth and zooplankton biomass between a historical and current stock–increase period in the western North Pacific. Fish. Res. **255**: 106461. doi:10.1016/j.fishres.2022.106461.

Kaplan, I., Brown, C., Fulton, E., Gray, I., Field, J., and Smith, A. 2013. Impacts of depleting forage species in the California Current. Environ. Conserv. **40**(4): 380–393. doi:10.1017/S0376892913000052.

Koehn, L.E., Essington, T.E., Marshall, K.N., Sydeman, W.J., Szoboszlai, A.I., and Thayer, J.A. 2017. Trade-offs between forage fish fisheries and their predators in the California Current. ICES J. Mar. Sci. **74**(9): 2448–2458. doi:10.1093/icesjms/fsx072.

Koehn, L.E., Siple, M.C., and Essington, T.E. 2021. A structured seabird population model reveals how alternative forage fish control rules benefit seabirds and fisheries. Ecol. Appl. **31**(7): e02401. doi:10.1002/eap.2401. PMID: 34218492.

Koenigstein, S., Jacox, M.G., Pozo Buil, M., Fiechter, J., Muhling, B.A., Brodie, S., et al. 2022. Population projections of Pacific sardine driven by ocean warming and changing food availability in the California Current. ICES J. Mar. Sci. fsac191. doi:10.1093/icesjms/fsac191.

Konar, M., Qiu, S., Tougher, B., Vause, J., Tlusty, M., Fitzsimmons, K., et al. 2019. Illustrating the hidden economic, social and ecological values of global forage fish resources. Resour. Conserv. Recycl. **151**: 104456. doi:10.1016/j.resconrec.2019.104456.

Kuriyama, P.T., Zwolinski, J.P., Hill, K.T., and Crone, P.R. 2020. Assessment of the Pacific sardine resource in 2020 for U.S. management in 2020-2021. U.S. Department of Commerce, NOAA Technical Memorandum NMFS-SWFSC-628.

Lindegren, M., and Checkley, D.M., Jr. 2013. Temperature dependence of Pacific sardine (*Sardinops sagax*) recruitment in the California Current ecosystem revisited and revised. Can. J. Fish. Aquat. Sci. **70**(2): 245–252. doi:10.1139/cjfas-2012-0211.

Lo, N.C., Macewicz, B.J., and Griffith, D.A. 2005. Spawning biomass of Pacific sardine (*Sardinops sagax*), from 1994–2004 off California. CalCOFI Rep. **46**: 93–112.

MacCall, A.D., Klingbeil, R.A., and Methot, R.D. 1985. Recent increased abundance and potential productivity of Pacific mackerel (*Scomber japonicus*). CalCOFI Rep. **26**: 119–129.

Marshall, K.M., Koehn, L.E., Levin, P.S., Essington, T.E., and Jensen, O.P. 2019. Inclusion of ecosystem information in US fish stock assessments suggests progress toward ecosystem-based fisheries management. ICES J. Mar. Sci. **76**(1): 1–9. doi:10.1093/icesjms/fsy152.

Maunder, M.N., and Thorson, J.T. 2019. Modeling temporal variation in recruitment in fisheries stock assessment: a review of theory and practice. Fish. Res. **217**: 71–86. doi:10.1016/j.fishres.2018.12.014.

McClatchie, S., Goericke, R., Auad, G., and Hill, K. 2010. Re-assessment of the stock–recruit and temperature–recruit relationships for Pacific sardine (*Sardinops sagax*). Can. J. Fish. Aquat. Sci. **67**(11): 1782–1790. doi:10.1139/F10-101.

McClatchie, S., Hendy, I.L., Thompson, A.R., and Watson, W. 2017. Collapse and recovery of forage fish populations prior to commercial exploitation. Geophys. Res. Lett. **44**(4): 1877–1885. doi:10.1002/2016GL071751.

McDaniel, J., Piner, K., Lee, H.H., and Hill, K. 2016. Evidence that the migration of the northern subpopulation of Pacific sardine (*Sardinops sagax*) off the west coast of the United States is age-based. PLoS ONE, **11**(11): e0166780. doi:10.1371/journal.pone.0166780. PMID: 27851805.

Methot, R.D., Jr., and Wetzel, C.R. 2013. Stock Synthesis: a biological and statistical framework for fish stock assessment and fishery management. Fish. Res. **142**: 86–99. doi:10.1016/j.fishres.2012.10.012.

Muhling, B.A., Brodie, S., Smith, J.A., Tommasi, D., Gaitan, C.F., Hazen, E.L., et al. 2020. Predictability of species distributions deteriorates under novel environmental conditions in the California Current System. Front. Mar. Sci. **7**: 589. doi:10.3389/fmars.2020.00589.

O'Leary, C.A., Thorson, J.T., Miller, T.J., and Nye, J.A. 2020. Comparison of multiple approaches to calculate time-varying biological reference points in climate-linked population–dynamics models. ICES J. Mar. Sci. **77**(3): 930–941. doi:10.1093/icesjms/fsz215.

PFMC. 1998. Amendment 8 (to the northern anchovy fishery management plan) incorporating a name change to: the coastal pelagic species fishery management plan. Pacific Fishery Management Council, Portland, OR.

PFMC. 2013. Report of the Pacific Sardine Harvest Parameters Workshop. Pacific Fishery Management Council, Portland, OR.

PFMC. 2016. Pacific Coast groundfish fishery management plan for the California, Oregon, and Washington Groundfish Fishery. Pacific Fishery Management Council, Portland, OR.

PFMC. 2022. Status of the Pacific coast coastal pelagic species fishery and recommended acceptable biological catches: stock assessment and fishery evaluation 2021. Pacific Fishery Management Council, Portland, OR.

Piet, G.J., and Rice, J.C. 2004. Performance of precautionary reference points in providing management advice on North Sea fish stocks. ICES J. Mar. Sci. **61**(8): 1305–1312. doi:10.1016/j.icesjms.2004.08.009.

Pikitch, E., Boersma, P.D., Boyd, I.L., Conover, D.O., Cury, P., Essington, T., et al. 2012. Little fish, big impact: managing a crucial link in ocean food webs. Lenfest Ocean Program. Washington, DC.

Pikitch, E.K., Rountos, K.J., Essington, T.E., Santora, C., Pauly, D., Watson, R., et al. 2014. The global contribution of forage fish to marine fisheries and ecosystems. Fish Fish. **15**: 43–64. doi:10.1111/faf.12004.

Pitcher, T.J., 1995. The impact of pelagic fish behaviour on fisheries. Sci. Mar. **59**(3–4): 295–306.

Pozo Buil, M., Jacox, M.G., Fiechter, J., Alexander, M.A., Bograd, S.J., Curchitser, E.N., et al. 2021. A dynamically downscaled ensemble of future projections for the California Current system. Front. Mar. Sci. **8**: 612874.

Punt, A.E., Butterworth, D.S., de Moor, C.L., De Oliveira, J.A., and Haddon, M. 2016a. Management strategy evaluation: best practices. Fish Fish. **17**(2): 303–334. doi:10.1111/faf.12104.

Punt, A.E., MacCall, A.D., Essington, T.E., Francis, T.B., Hurtado-Ferro, F., Johnson, K.F., et al. 2016b. Exploring the implications of the harvest control rule for Pacific sardine, accounting for predator dynamics: a MICE model. Ecol. Model. **337**: 79–95. doi:10.1016/j.ecolmodel.2016.06.004.

R Core Team. 2022. R: a language and environment for statistical computing. R Foundation for Statistical Computing, Vienna, Austria. Available from https://www.R-project.org/ [accessed 6 October 2023].

Renfree, J.S., Beittel, A., Bowlin, N.M., Erisman, B.E., James, K., Mau, S.A., et al. 2023. Report on the Summer 2022 California Current Ecosystem Survey (CCES) (2207RL), 27 June to 30 September 2022, conducted aboard NOAA ship Reuben Lasker, fishing vessels Lisa Marie and Long Beach Carnage, and uncrewed surface vehicles. NOAA technical memorandum NMFS NOAA-TM-NMFS-SWFSC; 678. doi:10.25923/66p9-hc28.

Rykaczewski, R.R., and Checkley, D.M., Jr. 2008. Influence of ocean winds on the pelagic ecosystem in upwelling regions. Proc. Natl. Acad. Sci. **105**(6): 1965–1970. doi:10.1073/pnas.0711777105.

Salvatteci, R., Field, D., Gutierrez, D., Baumgartner, T., Ferreira, V., Ortlieb, L., et al. 2018. Multifarious anchovy and sardine regimes in the Humboldt Current System during the last 150 years. Glob. Chang. Biol. **24**(3): 1055–1068. doi:10.1111/gcb.13991.

Schwartzlose, R.A., Alheit, J., Bakun, A., Baumgartner, T.R., Cloete, R., Crawford, R.J.M., et al. 1999. Worldwide large-scale fluctuations of sardine and anchovy populations. Afr. J. Mar. Sci. **21**: 289–347. doi:10.2989/025776199784125962.

Siple, M.C., Essington, T.E., and Plagányi, E.É. 2019. Forage fish fisheries management requires a tailored approach to balance trade-offs. Fish Fish. **20**(1): 110–124. doi:10.1111/faf.12326.

Siple, M.C., Koehn, L.E., Johnson, K.F., Punt, A.E., Canales, T.M., Carpi, P., et al. 2021. Considerations for management strategy evaluation for small pelagic fishes. Fish Fish. **22**(6): 1167–1186. doi:10.1111/faf.12579.

Stierhoff, K.L., Zwolinski, J.P., and Demer, D.A. 2020. Distribution, biomass, and demography of coastal pelagic fishes in the California Current ecosystem during summer 2019 based on acoustic-trawl sampling. In NOAA technical memorandum NMFS NOAA-TM-NMFS-SWFSC; 626. doi: 10.25923/nghv-7c40.

Szuwalski, C.S., and Hilborn, R. 2015. Environment drives forage fish productivity. Proc. Natl. Acad. Sci. **112**(26): E3314–E3315. doi:10.1073/pnas.1507990112.

Tommasi, D., Stock, C.A., Hobday, A.J., Methot, R., Kaplan, I.C., Eveson, J.P., et al. 2017. Managing living marine resources in a dynamic environment: the role of seasonal to decadal climate forecasts. Prog. Oceanogr. **152**: 15–49. doi:10.1016/j.pocean.2016.12.011.

Uriarte, A., Ibaibarriaga, L., Sánchez-Maroño, S., Abaunza, P., Andrés, M., Duhamel, E., et al. 2023. Lessons learnt on the management of short-lived fish from the Bay of Biscay anchovy case study: satisfying fishery needs and sustainability under recruitment uncertainty. Mar. Pol. **150**: 105512. doi:10.1016/j.marpol.2023.105512.

Wolf, P., and Smith, P.E. 1985. An inverse egg production method for determining the relative magnitude of Pacific sardine spawning biomass off California. CalCOFI Rep. **26**: 130–138.

Zwolinski, J.P., and Demer, D.A. 2012. A cold oceanographic regime with high exploitation rates in the Northeast Pacific forecasts a collapse of the sardine stock. Proc. Natl. Acad. Sci. **109**(11): 4175–4180. doi:10.1073/pnas.1113806109.

Zwolinski, J.P., and Demer, D.A. 2014. Environmental and parental control of Pacific sardine (*Sardinops sagax*) recruitment. ICES J. Mar. Sci. **71**(8): 2198–2207. doi:10.1093/icesjms/fst173.

Zwolinski, J.P., and Demer, D.A. 2019. Re-evaluation of the environmental dependence of Pacific sardine recruitment. Fish. Res. **216**: 120–125. doi:10.1016/j.fishres.2019.03.022.

Zwolinski, J.P., Emmett, R.L., and Demer, D.A. 2011. Predicting habitat to optimize sampling of Pacific sardine (*Sardinops sagax*). ICES J. Mar. Sci. **68**(5): 867–879. doi:10.1093/icesjms/fsr038.